Modelling the suction-and deviator stress-dependent resilient modulus of unsaturated fine/coarse soil mixture by considering soil-water retention curve

Yu Su, Yu-Jun Cui

Modelling the suction- and deviator stress-dependent resilient modulus of unsaturated fine/coarse soil mixture by considering soil-water retention curve

Yu Su[1,2], Yu-Jun Cui[2], Jean-Claude Dupla[2], Jean Canou[2]

1: School of Civil Engineering and Architecture, Nanchang University, Nanchang 330031, China

2: Laboratoire Navier/CERMES, Ecole des Ponts ParisTech (ENPC), France

Corresponding author

Yu SU

1. School of Civil Engineering and Architecture, Nanchang University, Nanchang 330031, China

2. Ecole des Ponts ParisTech, Laboratoire Navier/CERMES, 6 – 8 av. Blaise Pascal, Cité Descartes, Champs-sur-Marne, 77455 Marne – la – Vallée cedex 2, France

E-mail address: yu.su@enpc.fr

Abstract

Experimental observations have shown that the resilient modulus M_r of fine/coarse soil mixture can be significantly affected by the coarse grain content f_v, deviator stress σ_d and suction ψ. In this study, a constitutive model incorporating the soil-water retention curve (SWRC) was proposed to describe the effects of ψ and σ_d on M_r. This model was then extended to the effect of f_v. The proposed model implied the resilient modulus at saturation condition ($M_{r\text{-}sat}$), the resilient modulus at optimum moisture content (OMC) condition ($M_{r\text{-}opt}$), the suction at OMC (ψ_{opt}) and the parameters related to SWRC. The model was validated using experimental data from five studies reported in literature. Comparisons with three representative existing models showed that the proposed model was capable to well describe the suction-dependent effect of deviator stress in the full range of suction, while the existing models gave satisfactory simulation results only in the low suction range. Indeed, experimental studies revealed that there was a threshold suction ψ_{th}, and with increasing σ_d, the M_r decreased when $\psi < \psi_{th}$, but increased when $\psi > \psi_{th}$. When $\psi < \psi_{th}$, all models gave good simulations. On the contrary, when $\psi > \psi_{th}$, only the proposed model gave good simulations, in particular when $\psi_{th} > \psi_{opt}$. This showed the performance of the proposed model in describing the variation of resilient modulus of unsaturated fine/coarse soil mixtures with changes in coarse grain content, deviator stress and suction.

Keywords: resilient modulus; constitutive model; suction; deviator stress; coarse grain content; soil-water retention curve

INTRODUCTION

An interlayer soil was naturally created in the French conventional rail tracks, corresponding to a mixture of ballast grains and subgrade fine soil. The in-situ investigation showed a decrease of ballast grain content over the depth of interlayer soil (Trinh [1]). The resilient modulus M_r, defined as the ratio of cyclic deviator stress to resilient strain, was adopted to characterize the stiffness of interlayer soil (Nie et al. [2]). Wang et al. [3 - 5] and Qi et al. [6] studied the effects of coarse grain content f_v (the ratio of the volume of micro-ballast grains to that of mixture) and deviator stress σ_d on M_r of interlayer soil by cyclic triaxial tests under constant suction ψ. Figs. 1(a)-(b) show the grain size distribution curves of fine soil and micro-ballast, among which the micro-ballast was fabricated by a mixture of three coarse grains G 4-10, HN 2-4 and G 10-20 (see more details in Wang et al. [3]). The effect of ψ on the M_r of interlayer soil was further investigated by Su et al. [7] through multi-stage deviator stresses cyclic tests. Those experimental results indicated that the M_r of such fine/coarse soil mixture was significantly affected by coarse grain content f_v, suction ψ and deviator stress σ_d. From a practical point of view, it appears important to develop a constitutive model of M_r for the fine/coarse soil mixture, taking the combined effects of f_v, ψ and σ_d into consideration.

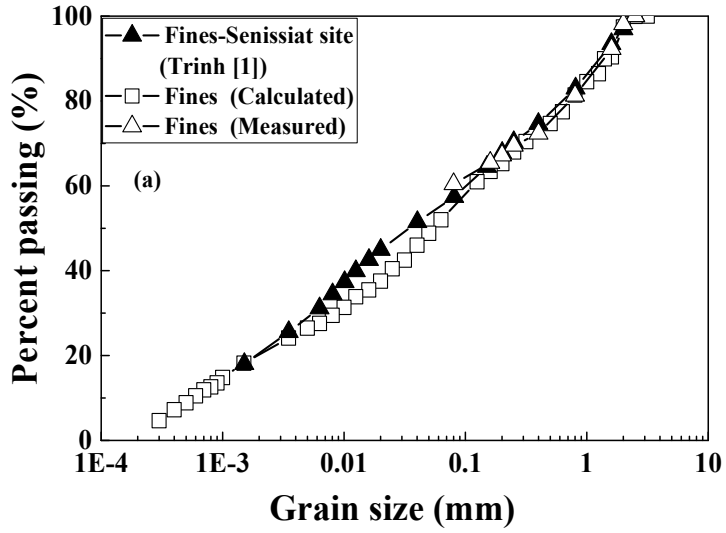

58

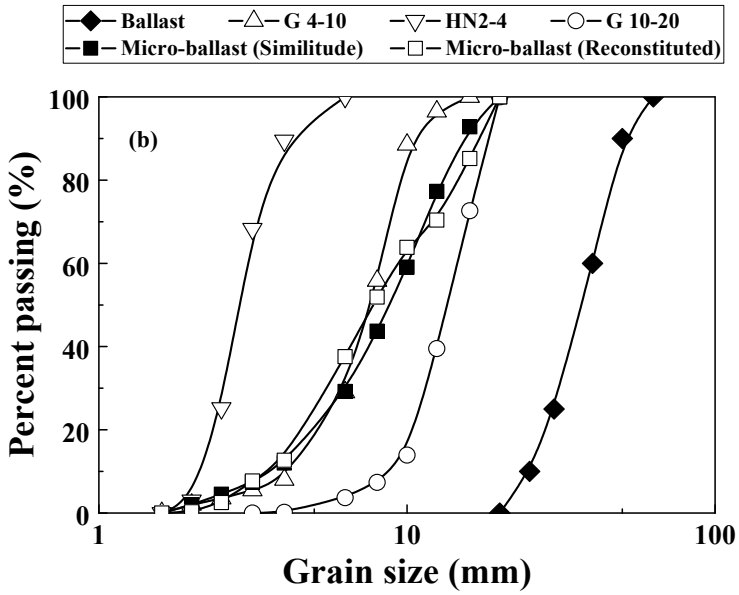

59

Fig. 1. Grain size distribution curves of (a) fine soil and (b) micro-ballast (after Wang et al. [3])

60 The effects of $f_{v,}$ ψ and σ_d on M_r were addressed in numerous experimental studies and

61 different models were proposed for that. Wang et al. [3] and Cui et al. [8] studied the effect of

62 f_v on the M_r of fine/coarse soil mixture, and defined a characteristic coarse grain content $f_{v\text{-cha}}$

63 separating two fabric kinds for the mixtures: a fine matrix macrostructure at $f_v \leq f_{v\text{-}cha}$, and a
64 coarse grain skeleton fabric at $f_v \geq f_{v\text{-}cha}$. They found that M_r increased slowly with increasing f_v
65 at $f_v \leq f_{v\text{-}cha}$, while quickly at $f_v \geq f_{v\text{-}cha}$. No constitutive model has been developed for describing
66 this phenomenon.

67 The effects of ψ and σ_d on M_r were generally investigated by multi-stage loadings cyclic
68 triaxial tests (Gupta et al. [9]; Nowamooz et al. [10]). Gu et al. [11] performed a series of
69 large-scale cyclic triaxial tests on unbound granular materials, and found that the increase in
70 both ψ and σ_d led to an increase of M_r. Ng et al. [12] studied the effects of ψ and σ_d on the M_r
71 of unsaturated subgrade soil by suction-controlled cyclic triaxial tests. The results showed that
72 in a narrow range of ψ from 0 to 250 kPa, an increase of ψ induced an increase of M_r, and an
73 increase of σ_d led to a reduction of M_r at a constant ψ. Yang et al. [13] performed suction-
74 controlled tests on residual mudstone soil with various deviator stresses σ_d. They reported that
75 with increasing σ_d, the M_r decreased at low suctions (ψ = 50 and 150 kPa), while increased at
76 a high suction (ψ = 450 kPa). Similarly, Su et al. [7] studied the effect of w on the M_r of
77 fine/coarse soil mixture through multi-stage loadings cyclic triaxial tests. They found that an
78 increase of w led to a decrease of M_r of soil mixture, due to the effect of ψ. Moreover, in the
79 case of low ψ (smaller than or equal to ψ_{opt} at optimum moisture content OMC), the increase
80 of σ_d resulted in a decrease of M_r, while in the case of high ψ (larger than ψ_{opt}), an opposite
81 trend was observed. Han and Vanapalli [14] investigated the effect of ψ on the M_r of
82 unsaturated subgrade soil, and proposed a constitutive model incorporating the soil-water
83 retention curve (SWRC). Oh et al. [15] and Han and Vanapalli [16 - 17] also consider SWRC

84 while modeling the effect of ψ on M_r. To date, there are no models for the description of M_r
85 variation with changes in ψ and σ_d for unsaturated fine/coarse soil mixtures.

86 In this study, a constitutive model of M_r was proposed for unsaturated fine/coarse soil
87 mixtures, accounting for the effects of ψ, σ_d, and f_v. Experimental data collected from
88 literature including the authors' own data were used to validate the model. Comparisons
89 between the proposed model and three representative existing models showed that the
90 proposed model is capable to well describe the variations of M_r with changes in σ_d and f_v in the
91 full range of ψ.

92

93 MODELLING BACKGROUND

94 Some investigators proposed empirical models to simulate the M_r - ψ relationship. For
95 instance, Sawangsuriya et al. [18] studied the effect of ψ on M_r with four compacted subgrade
96 soils, and proposed Eqs. (1) - (2) by considering two reference M_r values at saturation
97 condition and OMC condition- $M_{r\text{-}sat}$ and $M_{r\text{-}opt}$, respectively:

98 $$M_r/M_{r-sat} = -5.61 + 4.54\log(\psi) \quad (1)$$

99 $$M_r/M_{r-opt} = -0.24 + 0.25\log(\psi) \quad (2)$$

100 Ba et al. [19] proposed Eq. (3) to estimate the variations of M_r of four compacted granular
101 materials with respect to ψ using a resilient modulus ratio of M_r to the $M_{r\text{-}opt}$:

102 $$M_r/M_{r-opt} = 0.385 + 0.267\log(\psi) \quad (3)$$

These empirical models were simple and their parameters could be easily determined by regression analysis. However, since they were generally derived from limited experimental data, it appears difficult to be generalized to other materials.

The Mechanistic-Empirical Pavement Design Guide (MEPDG) (ARA, Inc., ERES Consultants Division. [20]) recommended the commonly used Eq. (4) to describe the variation of M_r with stress:

$$M_r = k_1 p_a \left(\frac{\theta_b}{p_a}\right)^{k_2} \left(\frac{\tau_{oct}}{p_a} + 1\right)^{k_3} \quad (4)$$

where θ_b is the bulk stress, equal to the sum of the three principal stresses σ_1, σ_2 and σ_3; τ_{oct} is the octahedral shear stress, equal to $\sqrt{2}/3(\sigma_1 - \sigma_3)$ in triaxial condition; p_a is the atmospheric pressure; k_1 , k_2 and k_3 are model parameters.

Liang et al. [21] studied the effects of stress state and suction on the M_r of cohesive soil. They proposed Eq. (5) by incorporating ψ into the bulk stress of Eq. (4) using the Bishop's effective stress parameter χ:

$$M_r = k_4 p_a \left(\frac{\theta_b + \chi\psi}{p_a}\right)^{k_5} \left(\frac{\tau_{oct}}{p_a} + 1\right)^{k_6} \quad (5)$$

where k_4, k_5 and k_6 are model parameters.

Similarly, Heath et al. [22] investigated the M_r of unsaturated granular materials, and developed Eq. (6) by modifying Eq. (4) using the Bishop's effective stress parameter χ:

$$M_r = k_7 p_a \left(\frac{\frac{\theta_b}{3} u_a + \chi\psi}{p_a}\right)^{k_8} \left(\frac{\sigma_d}{p_a}\right)^{k_9} \quad (6)$$

where k_7, k_8 and k_9 are model parameters; u_a is the pore air pressure.

Gupta et al. [9] and Khoury et al. [23] modified Eq. (4) by adding ψ as an independent term, such as $A\psi^B$ in Eqs. (7) and (8) for subgrade soils:

$$M_{\mathrm{r}} = k_{10} p_{\mathrm{a}} \left(\frac{\theta_{\mathrm{b}} - 3k_{11}}{p_{\mathrm{a}}}\right)^{k_{12}} \left(\frac{\tau_{\mathrm{oct}}}{p_{\mathrm{a}}} + k_{13}\right)^{k_{14}} + A_1 \psi^{B_1} \quad (7)$$

$$M_{\mathrm{r}} = k_{15} p_{\mathrm{a}} \left(\frac{\theta_{\mathrm{b}}}{p_{\mathrm{a}}}\right)^{k_{16}} \left(\frac{\tau_{\mathrm{oct}}}{p_{\mathrm{a}}} + k_{17}\right)^{k_{18}} + A_2 \psi^{B_2} \quad (8)$$

where k_{10}–k_{18}, A_1, B_1, A_2 and B_2 are model parameters.

The MEPDG (ARA, Inc., ERES Consultants Division. [20]) adopted Eq. (9) to predict the variation of M_{r} with respect to the seasonal variation of water content in the field condition:

$$\log\left(\frac{M_{\mathrm{r}}}{M_{\mathrm{r-opt}}}\right) = a + \frac{b-a}{1+\exp\left[\ln\frac{-b}{a} + k_{\mathrm{m}} \cdot (S_{\mathrm{r}} - S_{\mathrm{r-opt}})\right]} \quad (9)$$

where S_{r} is the degree of saturation; $M_{\mathrm{r\text{-}opt}}$ and $S_{\mathrm{r\text{-}opt}}$ are the resilient modulus and the degree of saturation at OMC, respectively; a and b are the minimum and maximum values of log ($M_{\mathrm{r}}/M_{\mathrm{r\text{-}opt}}$), respectively; k_{m} is a regression parameter. For fine-grained soil, a = -0.5934, b = 0.4 and k_{m} = 6.1324; for coarse-grained soil, a = -0.3123, b = 0.3 and k_{m} = 6.8157.

Han and Vanapalli [14] proposed Eq. (10) for compacted subgrade fine soils, incorporating SWRC:

$$\frac{M_{\mathrm{r}} - M_{\mathrm{r-sat}}}{M_{\mathrm{r-opt}} - M_{\mathrm{r-sat}}} = \frac{\psi}{\psi_{\mathrm{opt}}} \left(\frac{S_{\mathrm{r}}}{S_{\mathrm{r-opt}}}\right)^{\xi} \quad (10)$$

where ξ is the model parameter.

Summarizing, Table 1 presents a summary of model parameters for Eqs. (1) - (10).

Table 1. A summary of parameters for Eqs. (1) - (10)

Reference	Equation	Model parameters
Sawangsuriya et al. [18]	(1)	ψ and $M_{r\text{-}sat}$
	(2)	ψ and $M_{r\text{-}opt}$
Ba et al. [19]	(3)	ψ and $M_{r\text{-}opt}$
ARA, Inc., ERES Consultants Division. [20]	(4)	θ_b, τ_{oct}, p_a, k_1, k_2 and k_3
Liang et al. [21]	(5)	θ_b, τ_{oct}, p_a, $\chi\psi$, k_4, k_5 and k_6
Heath et al. [22]	(6)	θ_b, p_a, $\chi\psi$, u_a, σ_d, k_7, k_8 and k_9
Gupta et al. [9]	(7)	θ_b, τ_{oct}, p_a, ψ, k_{10}, k_{11}, k_{12}, k_{13}, A_1 and B_1
Khoury et al. [23]	(8)	θ_b, τ_{oct}, p_a, ψ, k_{15}, k_{16}, k_{17}, k_{18}, A_2 and B_2
ARA, Inc., ERES Consultants Division. [20]	(9)	S_r, $S_{r\text{-}opt}$, $M_{r\text{-}opt}$, a, b and k_m
Han and Vanapalli [14]	(10)	S_r, $S_{r\text{-}opt}$, $M_{r\text{-}opt}$, $M_{r\text{-}sat}$ and ξ

PROPOSITION OF A NEW MODEL

Proposing a model accounting for the effects of ψ and σ_d

Han and Vanapalli [17] reviewed the existing constitutive models of M_r with respect to ψ, and proposed a general form as follows:

$$M_r = M_{r-sat} + f(\psi),\ f(0) = 0 \tag{11}$$

where function $f(\psi)$ represents the contribution of ψ to M_r.

Referring to the existing models (e.g. Eq. (5) in Liang et al. [21] and Eq. (6) in Heath et al. [22]), a factor $\chi\psi$ was adopted to reflect the effect of ψ on the M_r of unsaturated soils. As stated by Han and Vanapalli [16], using factor $\chi\psi$ induced a change of the role of suction ψ from a pore-scale stress to a macroscopic stress which contributed to the constitutive stress and hence the M_r of unsaturated soils. In this study, factor $\chi\psi$ was modified by considering (*i*)

155 a power relationship of M_r - ψ in Eqs. (7) - (8) (Gupta et al. [9] and Khoury et al. [23]) and (*ii*)
156 a parameter χ equal to the effective degree of saturation S_r^e, which was defined as the ratio of
157 $(S_r - S_{r-r})$ to $(1 - S_{r-r})$, where $S_{r\text{-}r}$ is the residual degree of saturation (Alonso et al. [24]; Lu
158 et al. [25]). Therefore, a new factor $\psi^B S_r^e$ was generated and Eq. (12) was obtained:

159 $$M_r = M_{r-sat} + A \cdot \psi^B \cdot S_r^e \quad (12)$$

160 where A and B are model parameters.

161 Substituting $M_{r\text{-}opt}$ and the corresponding ψ_{opt} and S_{r-opt}^e (the effective degree of
162 saturation at OMC) into Eq. (12) yields Eq. (13):

163 $$M_{r-opt} = M_{r-sat} + A \cdot \psi_{opt}^B \cdot S_{r-opt}^e \quad (13)$$

164 Dividing Eq. (12) by Eq. (13) leads to the normalized Eq. (14) where parameter A
165 vanishes:

166 $$\frac{M_r - M_{r-sat}}{M_{r-opt} - M_{r-sat}} = \left(\frac{\psi}{\psi_{opt}}\right)^B \cdot \frac{S_r^e}{S_{r-opt}^e} \quad (14)$$

167 Eq. (15) (Moossazadeh and Witczak [26]) was commonly used to characterize the effect
168 of σ_d on M_r. Based on Eq. (15), Eq. (16) was proposed for relating σ_d to parameter B in Eq.
169 (14):

170 $$M_r = k_{19}\left(\frac{\sigma_d}{p_a}\right)^{k_{20}} \quad (15)$$

171 $$B = l_1 \cdot \left(\frac{\sigma_d}{p_a}\right)^{l_2} \quad (16)$$

172 where k_{19}, k_{20}, l_1 and l_2 are model parameters.

173 The van Genuchten [27] model was adopted for describing the SWRC:

$$S_r^e = \frac{S_r - S_{r-r}}{1 - S_{r-r}} = \left[\frac{1}{1+(a\psi)^n}\right]^m \quad (17)$$

where $S_{r\text{-}r}$ is the residual degree of saturation, assumed to be 0 in this study; a, n and m are model parameters.

Substituting Eqs. (16) and (17) into Eq. (14), Eq. (18) was obtained, which allowed prediction of the variation of M_r under the combined effects of ψ and σ_d:

$$\frac{M_r - M_{r-sat}}{M_{r-opt} - M_{r-sat}} = \left(\frac{\psi}{\psi_{opt}}\right)^{l_1 \cdot \left(\frac{\sigma_d}{p_a}\right)^{l_2}} \cdot \left[\frac{1+(a\psi_{opt})^n}{1+(a\psi)^n}\right]^m \quad (18)$$

Note that when ψ represented the matric suction, ψ_{opt} was the matric suction at optimum water content (e.g. for soils 1-5 in Table 2 and soils 6-9 in Table 3). On the contrary, when ψ represented the total suction, ψ_{opt} was the total suction at optimum water content (e.g. for soils 10-12 in Table 3). The matric suction was measured using the filter paper in contact with soil (for soils 1-8) or a thermal dissipation sensor (for soil 9), while the total suction was measured using a suction probe (for soil 10) or the filter paper without contact with soil (for soils 11-12).

Table 2 shows the properties of soils 1 - 5 tested by Wang et al. [3] and Su et al. [7], with f_v varying from 0% to 45%. Fig. 2 shows that the same SWRC was obtained for f_v = 0%, 20% and 35% using the filter paper method (Su et al. [28]). This indicated that an increase of f_v led to a constant ψ under a given S_r when keeping the dry density of fine soil constant ($\rho_{dmax\text{-}f}$ = 1.82 Mg/m^3 in Table 2), as expected by Wang et al. [3 - 5] and Qi et al. [6]. Fig. 3 shows the comparisons between the measurements by Wang et al. [3] and Su et al. [7] and the calculations by Eq. (18) for the variations of M_r with ψ under different deviator stresses σ_d and five f_v values. It can be observed from Fig. 3(a) that M_r increased with the increase of ψ under a constant σ_d, and a reasonably good agreement was obtained between the

measurements and the calculations. Further examination showed that a threshold suction ψ_{th} could be identified, corresponding to the intersection of the curves of different deviators stresses (σ_d = 50, 100 and 200 kPa). When $\psi < \psi_{th}$, the M_r decreased with increasing σ_d, while an opposite trend was observed when $\psi > \psi_{th}$. In addition, the increase of σ_d led to a decrease of model parameter l_1, keeping parameter l_2 constant (equal to 1.000). The similar phenomenon was observed in Figs. 3(b) - (e) for f_v = 10% - 45%. It seems that the higher the ψ_{th}, the higher the coefficient of determination R^2 for soils 1-5. Overall, a good agreement was obtained between measurements and calculations, with the $R^2 \geq 0.90$. Figs. 3(a) - (e) indicate that an increase of f_v from 0% to 45% resulted in an increase of $M_{r\text{-}sat}$ from 11 to 85 MPa.

Table 2. Soil properties in Wang et al. [3] and Su et al. [7]

Soil No.	f_v (%)	Fine soil fraction							USCS classification	Soil mixture	
		G_s	w_L (%)	w_p (%)	I_P (%)	$w_{opt\text{-}f}$ (%)	$\rho_{dmax\text{-}f}$ (Mg/m^3)	$S_{r\text{-}opt}$ (%)		Compaction $w_{opt\text{-}f}$ (%)	ρ_d (Mg/m^3)
1	0										1.82
2	10										1.91
3	20	2.68	32	12	20	13.7	1.82	78	CL	13.7	1.99
4	35										2.12
5	45										2.21

Note: f_v represents the ratio of the volume of coarse grains to that of mixture (Su et al. [7]). G_s, w_L, I_P, $w_{opt\text{-}f}$ and $\rho_{dmax\text{-}f}$ represent the specific gravity, liquid limit, plasticity index, optimum water content and maximum dry density of fine soil, respectively. $w_{opt\text{-}f}$ and $\rho_{dmax\text{-}f}$ were determined by standard Proctor compaction tests for soils 1-5. ρ_d represents the dry density of

soil mixture sample. USCS refers to the unified soil classification system: CL, low-plasticity clay; CH, high-plasticity clay; MH, high-plasticity silt; ML, low-plasticity silt.

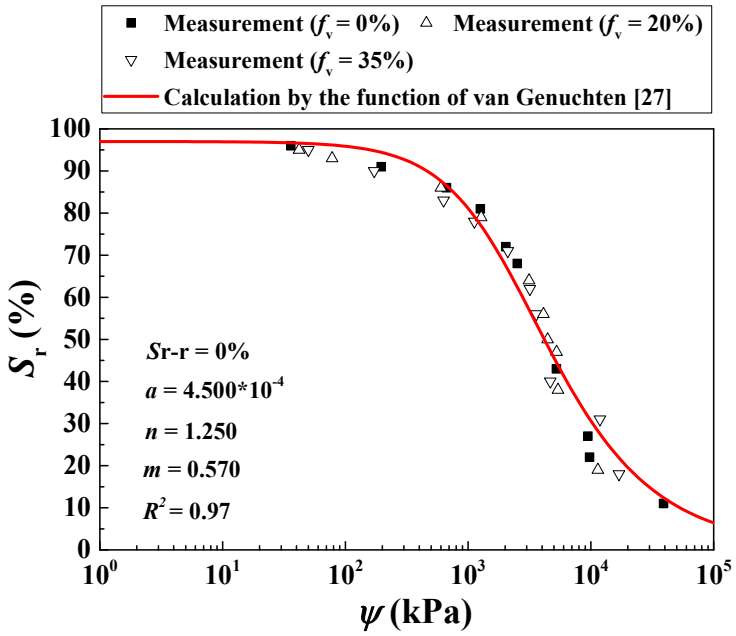

Fig. 2. Measured and calculated soil-water retention curves at varying f_v values for soils 1-5 (after Su et al. [28])

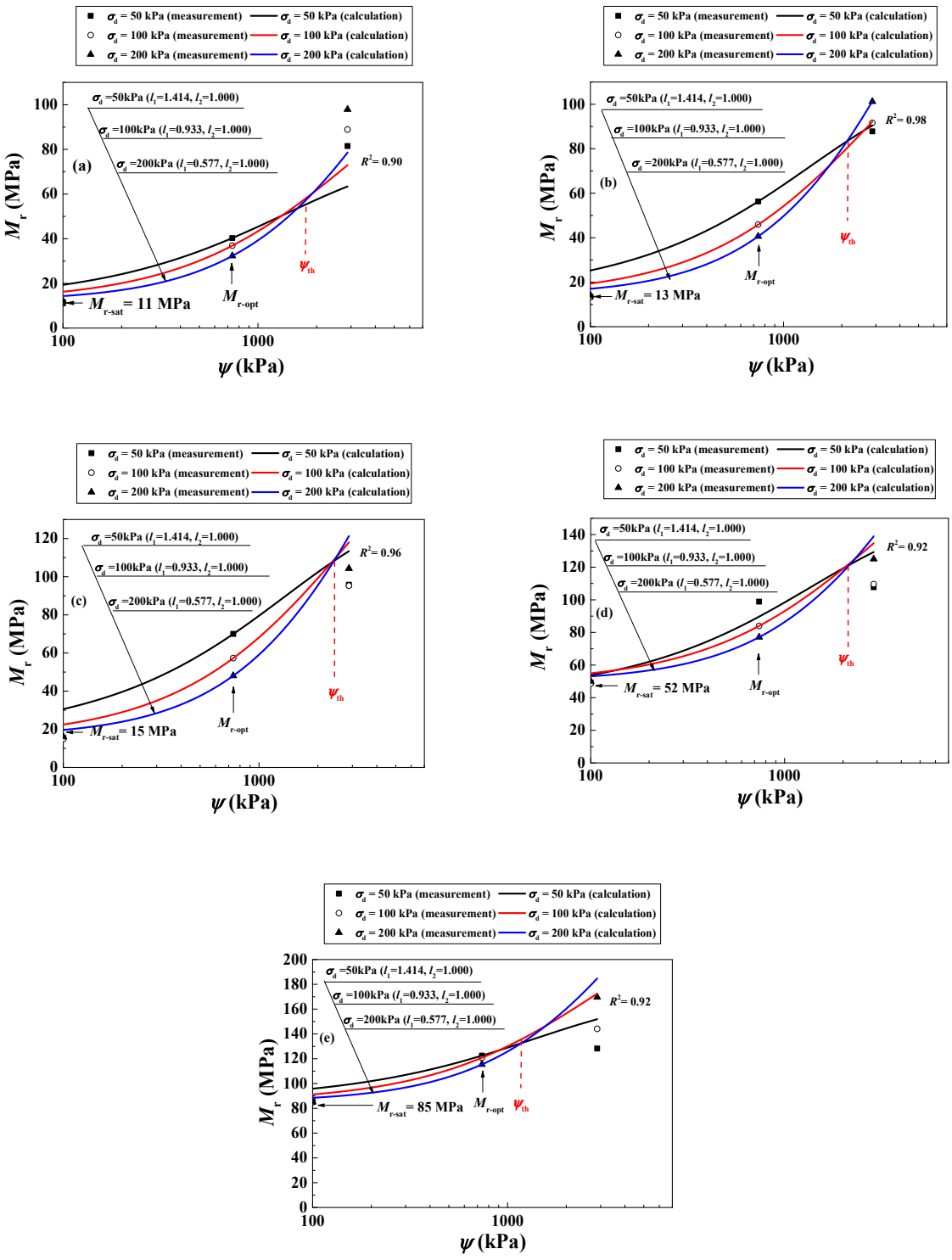

Fig. 3. Measured and calculated variations of M_r with ψ under varying σ_d for soils 1-5: (a) soil 1 at f_v = 0%; (b) soil 2 at f_v = 10%; (c) soil 3 at f_v = 20%; (d) soil 4 at f_v = 35%; (e) soil 5 at f_v = 45% (data from Wang et al. [3] and Su et al. [7])

231 The M_r - σ_d relationship depended on the combined effects of the soil hardening in the
232 loading process and the rebounding in the unloading process. When $\psi < \psi_{th}$, a matrix
233 structure of fine soil was expected due to the effect of water hydration (Su et al. [29]). On the
234 contrary, the high ψ induced an aggregated fine soil microstructure (Cui and Delage [30]; Ng
235 et al. [31]). Upon loading, an increase of σ_d contributed to the compression of fine matrix and
236 the rearrangement of fine aggregates (Werkmeister et al. [32]). Thus, an increase of M_r is
237 expected for both fabrics due to the hardening phenomenon. Conversely, in the unloading
238 process, owing to the rebounding effect, the resilient strain increased, which resulted in a
239 decrease of M_r. For the fine matrix fabric ($\psi < \psi_{th}$), due to its larger deformability, the effect
240 of rebounding on M_r appeared to be more significant than the effect of hardening, leading to a
241 decrease of M_r with increasing σ_d. By contrast, for the aggregated fabric ($\psi > \psi_{th}$), owing to
242 its lower deformability, the rebounding effect was not as significant as the hardening effect. In
243 this case, the M_r increased with increasing σ_d. This indicated that ψ_{th} could be considered as
244 the threshold value between the fine matrix fabric (at $\psi < \psi_{th}$) and the fine aggregate fabric (at
245 $\psi > \psi_{th}$). It appeared that ψ_{th} was slightly affected by the coarse grain content f_v. At f_v = 0% -
246 20%, a fine matrix macrostructure was obtained for soils 1 - 3, while at f_v = 35% - 45% the
247 coarse grains were dominant for soils 4 - 5. With increasing f_v, the transition of these two
248 fabrics contributed to a slight decrease of ψ_{th}, for that less fine soil was needed to be
249 transferred from the fine matrix fabric to the fine aggregate fabric.

250 Fig. 4 shows the variations of M_r with f_v under varying ψ and a constant σ_d = 200 kPa for
251 soils 1-5. Fig. 5 shows a linear variation of parameter l_1 with log (σ_d/p_a), leading to Eq. (19):

$$l_1 = \alpha_1 \log\left(\frac{\sigma_d}{p_a}\right) + \beta_1 \quad (19)$$

where α_1 and β_1 are model parameters. Eq. (19) allows the determination of the two parameters (α_1 = -1.390, β_1 = 0.967) with a regression coefficient R^2 = 0.99.

Substituting Eq. (19) into Eq. (18) yields Eq. (20):

$$\frac{M_r - M_{r-sat}}{M_{r-opt} - M_{r-sat}} = \left(\frac{\psi}{\psi_{opt}}\right)^{[\alpha_1 \log\left(\frac{\sigma_d}{p_a}\right) + \beta_1] \cdot \left(\frac{\sigma_d}{p_a}\right)} \cdot \left[\frac{1+(a\psi_{opt})^n}{1+(a\psi)^n}\right]^m \quad (20)$$

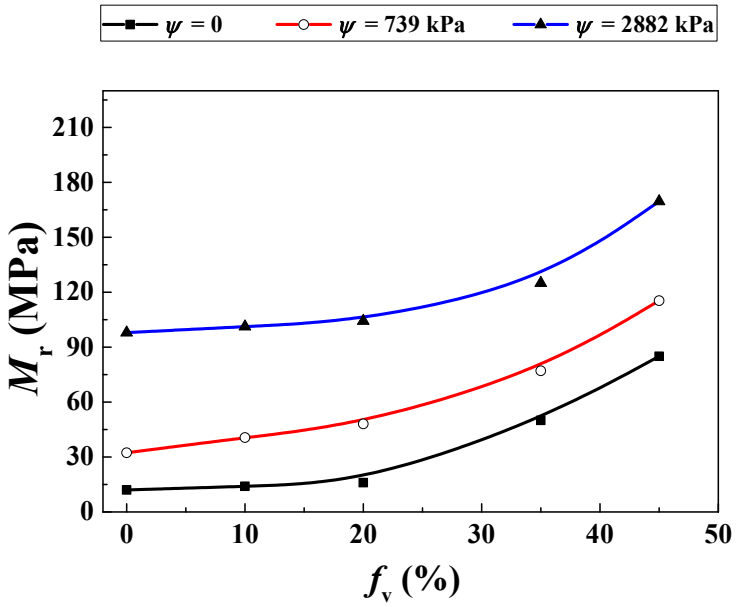

Fig. 4 Variations of M_r with f_v under varying ψ and a constant σ_d = 200 kPa for soils 1-5 (data from Wang et al. [3] and Su et al. [7])

Extending the model to the effect of f_v

Fig. 6 shows the variation of $M_{r\text{-}sat}$ with f_v, measured by Su et al. [7] and Duong et al. [33]. Note that the same fine soil fraction was adopted by Su et al. [7] and Duong et al. [33], while the micro-ballast was adopted by Su et al. [7] as a substitute of ballast adopted by Duong et al.

265 [33] following the parallel gradation method. The validity of this method was verified by Qi et
266 al. [34]. Since an increase of f_v led to a constant ψ under a given S_r (Fig. 2), the term $f(\psi)$ was
267 independent of f_v in Eq. (11). Similarly, the whole term on the right-hand side of Eq. (20) was
268 also independent of f_v. The effect f_v was reflected on the term $M_{r\text{-}sat}$ in Eqs. (11) and (20). It
269 was found from Figs. 3(a) - (e) (Wang et al. [3] and Su et al. [7]) that an increase of f_v from
270 0% to 45% resulted in an increase of $M_{r\text{-}sat}$ from 11 to 85 MPa. This $M_{r\text{-}sat}$ - f_v relationship was
271 expressed by Eq. (21):

272 $$M_{r-sat} = M_0 + \frac{M_1 - M_0}{1 + e^{k f_v + l}} \quad (21)$$

273 where M_0 and M_1 are the values of $M_{r\text{-}sat}$ at f_v = 0% and 100%, respectively; k and l are model
274 parameters. Eq. (21) provides good simulations of $M_{r\text{-}sat}$ - f_v relationship measured by Duong
275 et al. [33] and Su et al. [7] with R^2 = 0.97, using parameters M_0 = 11 MPa, M_1 = 200 MPa, k =
276 -0.163 and l = 7.514.

277 It appears from Fig. 6 that the $M_{r\text{-}sat}$ - f_v curve could be divided into three zones with two
278 critical f_v values: a fine matrix macrostructure zone at $f_v < f_{v1}$, a transition zone at $f_{v1} < f_v < f_{v2}$
279 and a coarse grain skeleton zone at $f_v > f_{v2}$. Vallejo and Mawby [35] studied the stiffness and
280 shear strength of sand and clay mixture, and found $f_{v1} \approx 26\%$ and $f_{v2} \approx 56\%$. Cui et al. [8],
281 Wang et al. [4] and Su et al. [36] investigated the mechanical behavior of fine/coarse soil
282 mixture subjected to monotonic and cyclic loadings, and defined a characteristic coarse grain
283 content $f_{v\text{-}cha} \approx 25\% \sim 33\%$. They found that a fine matrix macrostructure was identified at $f_v \leq$
284 $f_{v\text{-}cha}$. Obviously, the $f_{v\text{-}cha}$ identified corresponded to f_{v1}.

285 Summarizing, Eqs. (20) - (21) allow the determination of the variation of M_r under the

286 combined effects of ψ, σ_d and f_v for the fine/coarse soil mixtures.

287

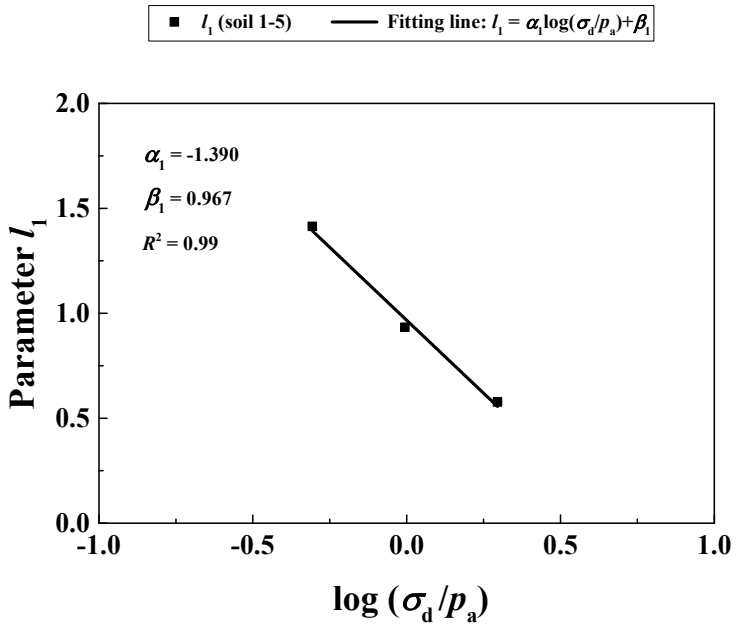

288

289 Fig. 5. Variation of parameter l_1 with log (σ_d/p_a) for soils 1-5

290

291

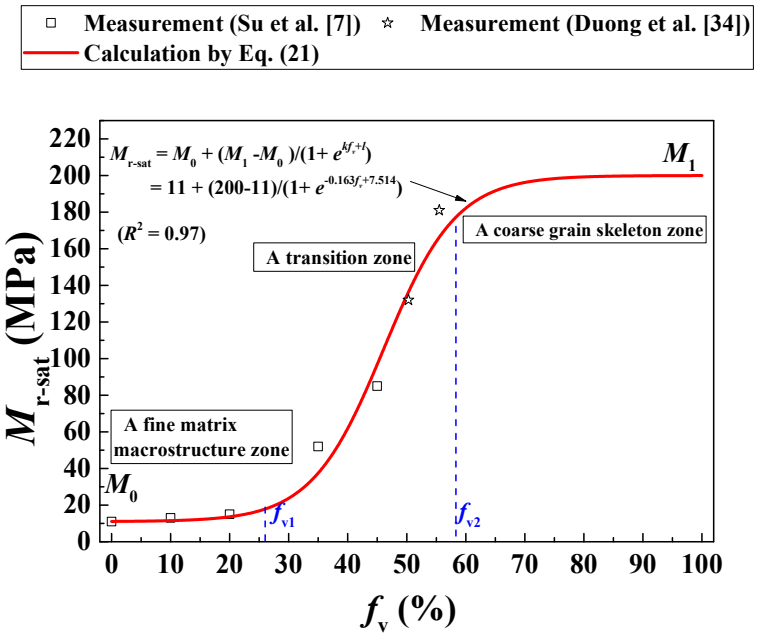

Fig. 6. Measured and calculated variation of $M_{r\text{-}sat}$ with f_v

VALIDATION OF THE PROPOSED MODEL

Table 3 shows the properties of soils 6 - 12 compiled from five different studies. As $f_v = 0\%$ in these studies, Eq. (21) was simplified to Eq. (22):

$$M_{r-sat} = M_0 \quad (22)$$

Soils 6 - 12 were divided into two categories. Category I included soils 6 - 8 (Zaman and Khoury [37]), soil 9 (Gupta et al. [9]) and soil 10 (Ng et al. [12]), for which M_r decreased with increasing σ_d under a given ψ. The ψ values considered were supposed to be smaller than ψ_{th}. Category II included soils 11 - 12 (Yang et al. [13], [38]), for which a value of ψ_{th} existed separating the ψ into two zones: with increasing σ_d, the M_r decreased at $\psi < \psi_{th}$ but increased at $\psi > \psi_{th}$. It is worth noting that ψ_{th} appeared soil type – dependent: smaller than ψ_{opt} for

soils 11 - 12 (Yang et al. [13], [38]) and larger than ψ_{opt} for soils 1 - 5 (Wang et al. [3]; Su et al. [7]). The plastic limit w_p can be helpful in explaining this phenomenon. With respect to the findings of Delage et al. [39], w_p was the threshold value between the fine matrix fabric and the fine aggregate fabric. For soils 1-5, the plastic limit w_p = 12% was smaller than $w_{opt\text{-}f}$ = 13.7% (Table 2), leading to $\psi_{th} > \psi_{opt}$. On the contrary, for soils 11-12, the w_p = 34% and 22% were larger than $w_{opt\text{-}f}$ = 18.1% and 16.8% respectively (Table 3), leading to $\psi_{th} < \psi_{opt}$.

Table 3. Soil properties in five different studies

Reference	Soil No.	f_v (%)	Fine soil fraction								Soil mixture	
			G_s	w_L (%)	w_p (%)	I_P (%)	$w_{opt\text{-}f}$ (%)	$\rho_{dmax\text{-}f}$ (Mg/m^3)	$S_{r\text{-}opt}$ (%)	USCS classification	Compaction w (%)	ρ_d (Mg/m^3)
Zaman and Khoury [37]	6		N/A	55	25	30	23.5	1.53	N/A	CH	19.5	1.53
	7										23.5	
	8										27.5	
Gupta et al. [9]	9	0	2.75	28	17	11	13.5	1.79	70	CL	13.5	1.79
Ng et al. [12]	10		2.73	43	29	14	16.3	1.76	80	ML	16.3	1.76
Yang et al. [38]	11		2.71	54	34	20	18.1	1.76	91	MH	18.1	1.76
Yang et al. [13]	12		2.67	37	22	15	16.8	1.77	88	CL	16.8	1.77

Note: $w_{opt\text{-}f}$ and $\rho_{dmax\text{-}f}$ were determined by standard Proctor compaction tests for soils 6-11, while modified Proctor compaction test for soils 12; N/A means data not available in the reference.

Zaman and Khoury [37] studied the effects of compaction water content and suction on M_r for Burleson soil (soils 6, 7 and 8 in Table 3). In their study, the soils were compacted at w = 19.5% (optimum water content of fine soil $w_{opt\text{-}f}$ - 4%), 23.5% ($w_{opt\text{-}f}$) and 27.5% ($w_{opt\text{-}f}$ + 4%) respectively and at the same maximum dry density of soil $\rho_{dmax\text{-}f}$ = 1.53 Mg/m^3. Cyclic triaxial tests were performed under a constant deviator stress σ_d = 28 kPa and a constant confining pressure σ_c = 41 kPa. The filter paper method was adopted to measure the suction ψ after completion of the cyclic tests. Fig. 7(a) shows the measured and calculated SWRCs for soils 6, 7 and 8 using Eq. (17) with the parameters shown in Table 4. The different SWRCs for soils 6, 7 and 8 were the consequences of their varying compaction water contents, as reported by Delage et al. [39] and Vanapalli et al. [40]. Figs. 7(b) - (d) depict the variations of M_r with ψ under σ_d = 28 kPa for soils 6, 7 and 8 respectively. Eq. (20) calculated the variations of M_r with ψ for these three soils using parameter α_1 = 0 and β_1 = 2.891. Comparisons between the measurements and calculations showed a good agreement (R^2 = 0.95).

Table 4. Parameters of SWRCs for soils 1-12

Soil No.	$S_{r\text{-}r}$ (%)	a	n	m	R^2	SWRC type
1 2 3 4	0	4.500*10^{-4}	1.250	0.570	0.97	Drying SWRC
5 6		1.770*10^{-3}	1.540	0.126	0.91	Apparent

7	$6.500 * 10^{-8}$	0.662	70.750	0.95	SWRC
8	$3.200 * 10^{-4}$	1.624	0.306	0.89	
9	$1.656 * 10^{-4}$	0.769	1.049	0.99	
10	$1.120 * 10^{-6}$	0.688	243.330	0.99	Drying SWRC
11	0.034	2.747	0.021	0.98	
12	0.139	0.779	0.197	0.98	

Note: Drying SWRC was obtained by following a desaturation path; Apparent SWRC was obtained by the S_r - ψ relationships determined after cyclic tests.

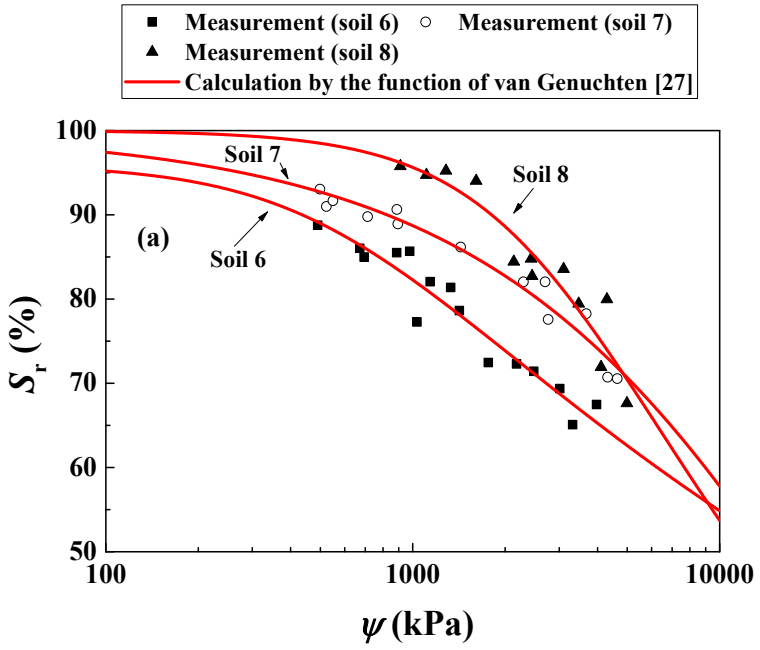
Measurement (soil 6)
Measurement (soil 7)
Measurement (soil 8)
Calculation by the function of van Genuchten [27]
(a)
Soil 7
Soil 8
Soil 6
S_r (%)
ψ (kPa)
100
90
80
70
60
50
100
1000
10000

337

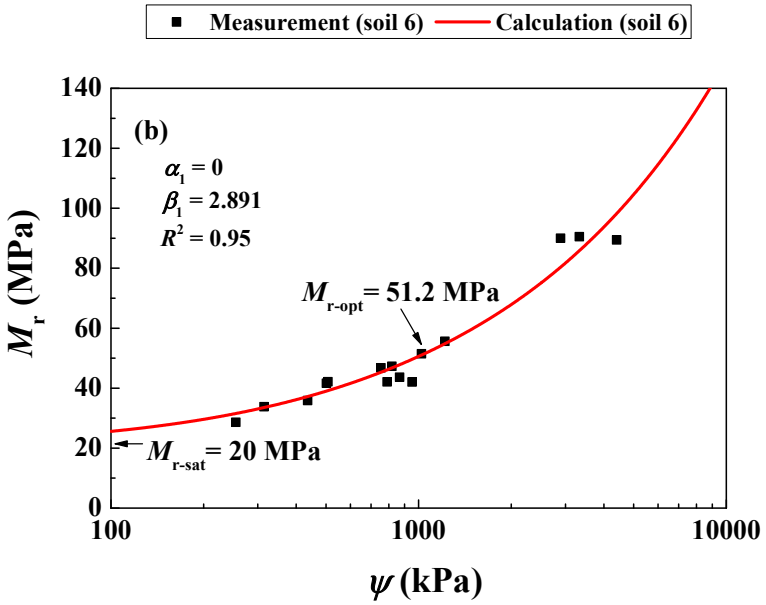
Measurement (soil 6)
Calculation (soil 6)
(b)
α_1 = 0
β_1 = 2.891
R^2 = 0.95
$M_{r\text{-}opt}$ = 51.2 MPa
$M_{r\text{-}sat}$ = 20 MPa
M_r (MPa)
ψ (kPa)
140
120
100
80
60
40
20
0
100
1000
10000

338

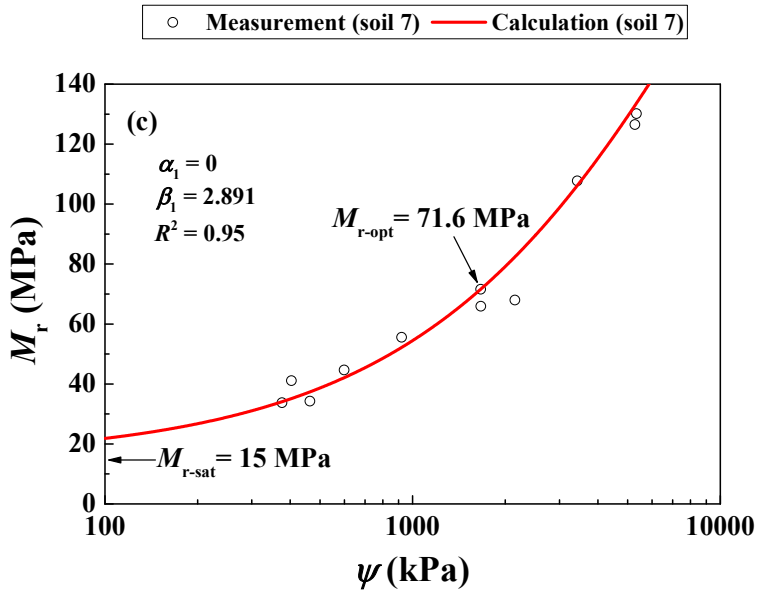

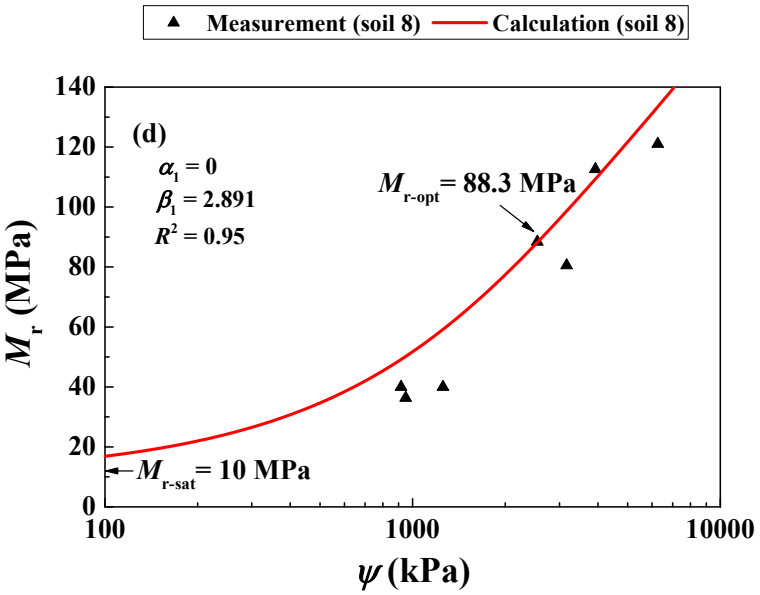

Fig. 7. Measured and calculated (a) SWRCs and (b)-(d) variations of M_r with ψ for soils 6-8 (data from Zaman and Khoury [37])

Gupta et al. [9] investigated the effects of ψ and σ_d on M_r of Duluth slope soil (soil 9 in Table 3). Soil 9 was compacted at $w_{opt\text{-}f}$ = 13.5% and $\rho_{dmax\text{-}f}$ = 1.79 Mg/m^3, defining a suction

347 ψ_{opt} = 245 kPa, which was measured using a thermal dissipation sensor. The compacted soil
348 was then subjected to a saturation process, followed by a drying process to different target
349 suctions. Cyclic triaxial tests were performed for the M_r measurement, with axis- translation
350 technique and a thermal dissipation sensor adopted for suction control and measurement. A
351 multi-stage loading with σ_d = 30, 50, 70 and 100 kPa was adopted under a constant σ_c = 14.5
352 kPa. Fig. 8(a) shows the measured and calculated SWRCs for soil 9 using Eq. (17). It appears
353 from Fig. 8(b) that M_r increased with increasing ψ under a constant σ_d, and the increase of σ_d
354 led to a decrease of M_r in the full measured ψ range. Eq. (20) provides the calculated results
355 using parameters α_1 = -2.808 and β_1 = 1.046. Comparisons between the measurements and
356 calculations showed a good agreement (R^2 = 0.98).

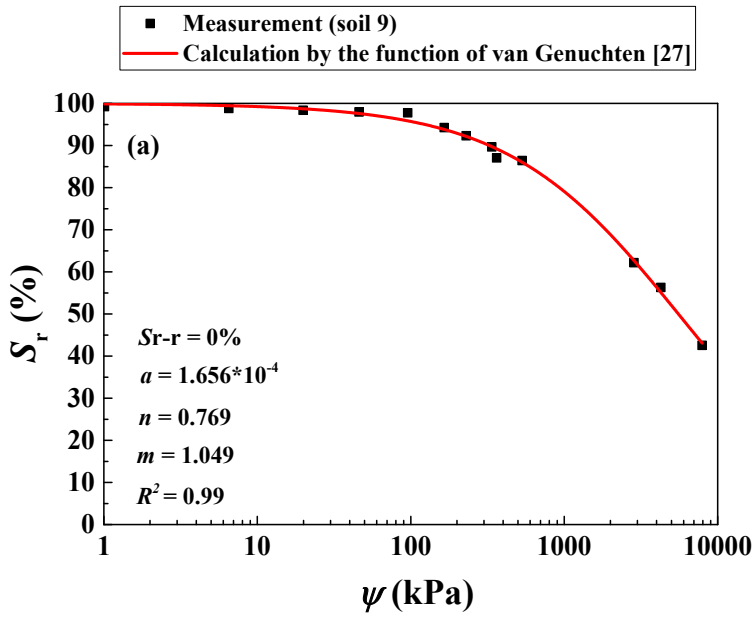

357

358

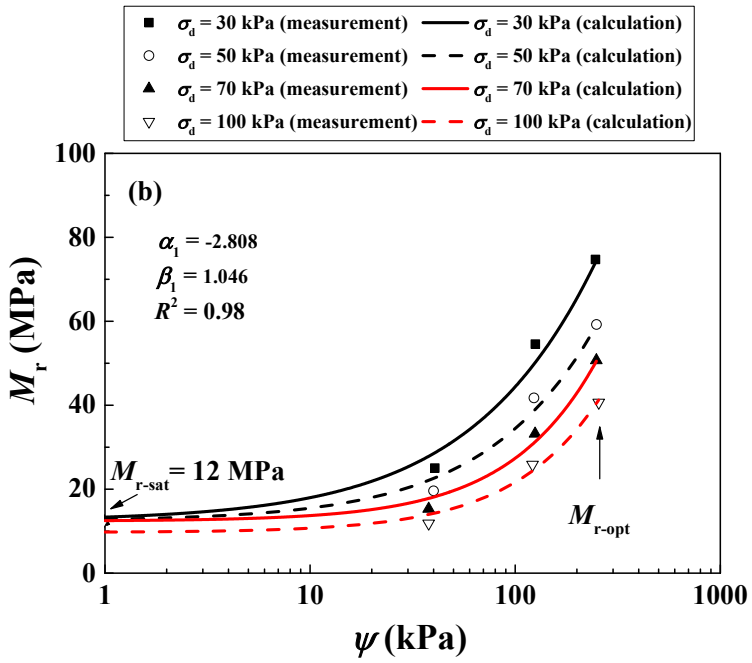

359

360 Fig. 8. Measured and calculated (a) SWRC and (b) variations of M_r with ψ for soil 9 (data
361 from Gupta et al. [9])

362

363 Ng et al. [12] investigated the variations of M_r with ψ under varying σ_d for a completely
364 decomposed tuff (soil 10 in Table 3). Soil 10 was compacted at $w_{opt\text{-}f}$ = 16.3% and $\rho_{dmax\text{-}f}$ =
365 1.76 Mg/m^3, and its corresponding ψ_{opt} = 95 kPa was measured by a suction probe. The
366 compacted soil was then wetted or dried to different target suctions. Suction-controlled cyclic
367 triaxial tests were performed under varying σ_d = 30, 40, 55 and 70 kPa and a constant σ_c = 30
368 kPa. Fig. 9(a) presents the measured and fitted SWRCs using Eq. (17). Fig. 9(b) depicts the
369 variations of M_r with ψ under varying σ_d measured by Ng et al. [12] and those calculated by
370 Eq. (20) using α_1 = -4.126 and β_1 = 1.535. A good agreement was observed between the
371 measurements and the calculations (R^2 = 0.96).

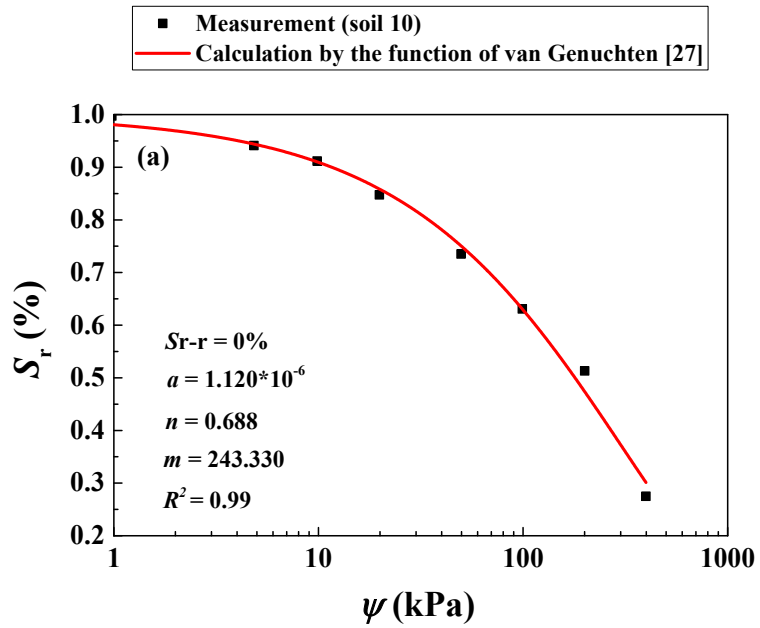

372

373

374

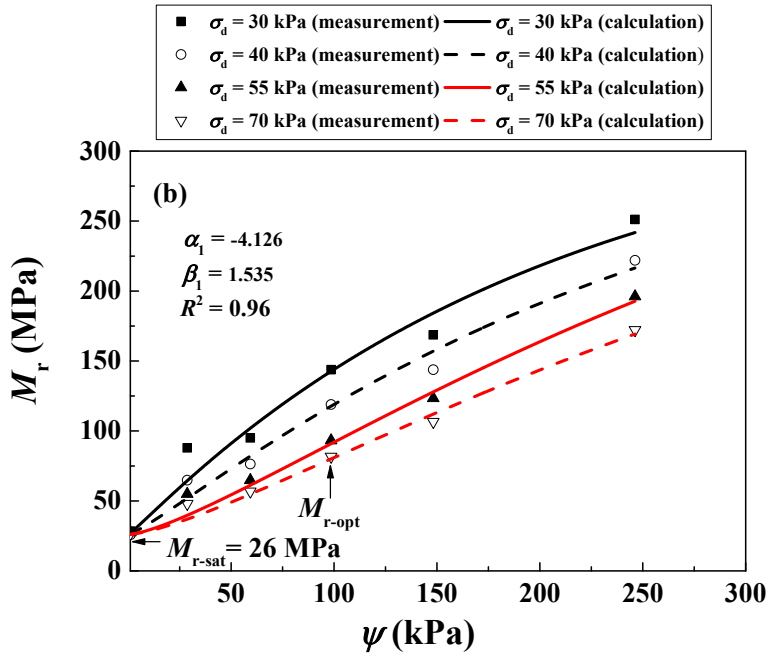

375

376 Fig. 9. Measured and calculated (a) SWRC and (b) variations of M_r with ψ for soil 10 (data
377 from Ng et al. [12])

378

379 Yang et al. [38] studied the variations of M_r with ψ under varying σ_d for a compacted
380 subgrade soil (soil 11 in Table 3). Soil 11 was compacted at $w_{opt\text{-}f}$ = 18.1% and $\rho_{dmax\text{-}f}$ = 1.76
381 Mg/m^3, with a suction ψ_{opt} = 5580 kPa measured using the filter paper method. The
382 compacted soil was then wetted to higher water contents (lower suctions). Cyclic triaxial tests
383 were performed under varying σ_d = 21, 34, 48, 69, 103 kPa and a constant σ_c = 21 kPa. After
384 completion of the tests, the filter paper method was applied to measure the suction ψ. Fig.
385 10(a) shows the SWRCs measured by Yang et al. [41] and fitted by Eq. (17). Fig. 10(b)
386 compares the measured M_r at different ψ and σ_d values and the corresponding calculated M_r
387 by Eq. (20) with parameters α_1 = -4.928 and β_1 = 0.681. A threshold suction ψ_{th} could be
388 identified, separating the ψ into two zones with different effects of σ_d.

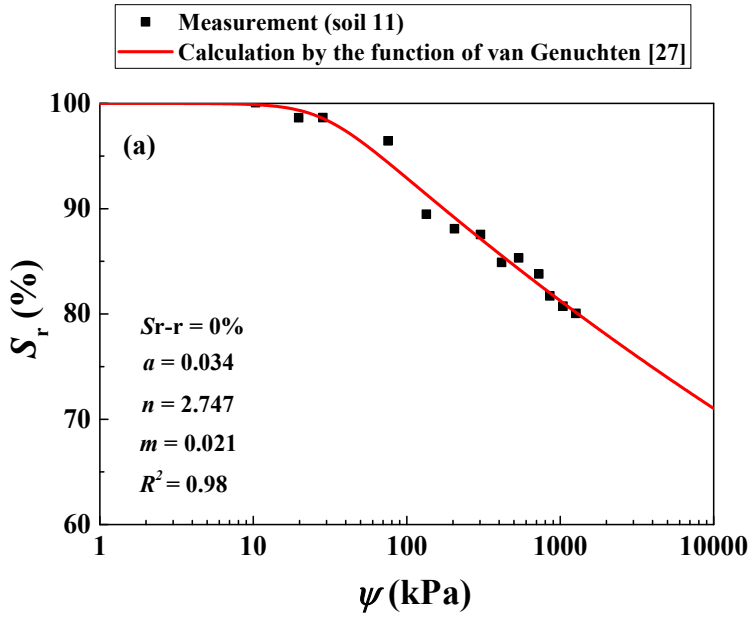

389

390

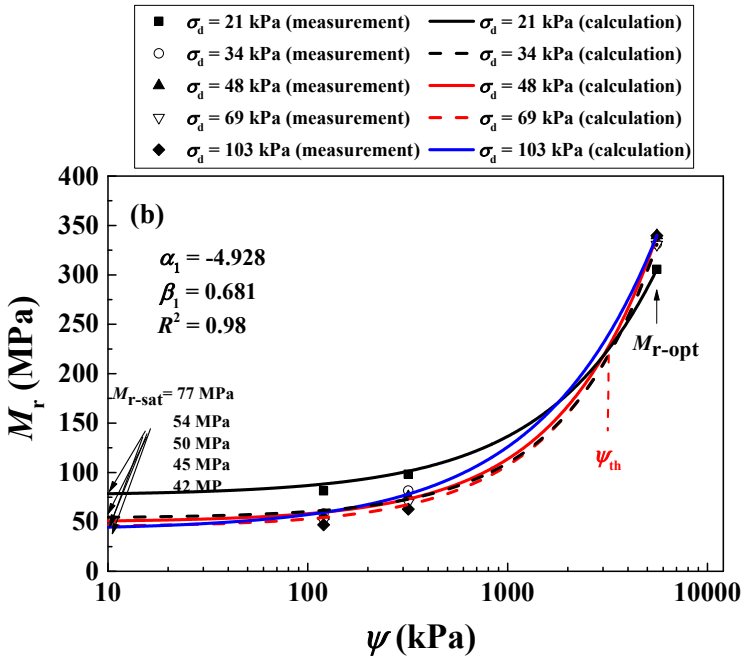

391

392 Fig. 10. Measured and calculated (a) SWRC (data from Yang et al. [41]) and (b) variations of
393 M_r with ψ for soil 11 (data from Yang et al. [38])

394

395 Yang et al. [13] investigated the variations of M_r with ψ under varying σ_d for a
396 compacted mudstone soil (soil 12 in Table 3). Soil 12 was compacted at $w_{opt\text{-}f}$ = 16.8% and
397 $\rho_{dmax\text{-}f}$ = 1.77 Mg/m^3, defining a suction ψ_{opt} = 500 kPa which was measured by the filter paper
398 method. It was then wetted to higher water contents (19.1%, 20.2% and 23.2%) to reach
399 various suctions (450, 150 and 50 kPa respectively). Cyclic triaxial tests were performed with
400 suction controlled by the axis-translation technique. Four deviator stresses σ_d = 34, 48, 69 and
401 103 kPa were applied in sequence under a constant σ_c = 21 kPa. Fig. 11(a) shows the
402 measured and fitted SWRCs by Eq. (17). Fig. 11(b) depicts the variations of M_r with ψ under
403 varying σ_d measured by Yang et al. [13] and those calculated by Eq. (20) with parameters α_1

= -3.943 and β_1 = 1.606. A ψ_{th} was identified from Fig. 11(b), separating the ψ into two zones with different effects of σ_d, which was consistent with the observation in Fig. 10(b).

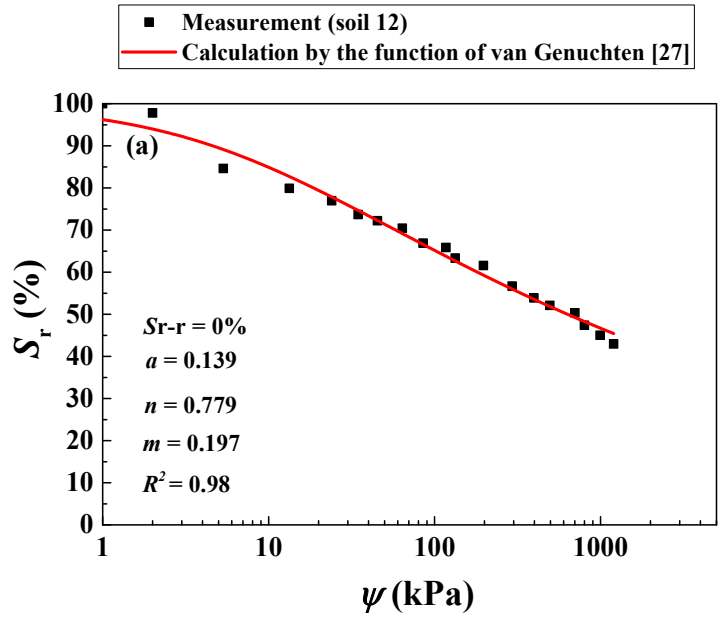

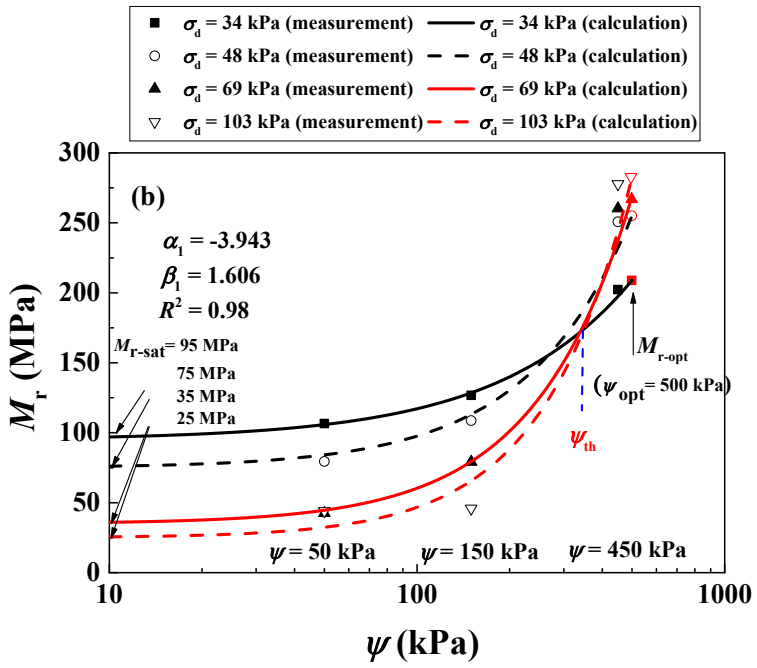

Fig. 11. Measured and calculated (a) SWRC and (b) variations of M_r with ψ for soil 12 (data from Yang et al. [13])

411 Table 5 presents the values of model parameters α_1 and β_1 in the proposed Eq. (20) for
412 soils 1-12, indicating that these parameters are dependent of soil studied. Fig. 12 shows the
413 comparison between the measured and the calculated M_r values using Eq. (20) for soils 1-12
414 listed in Tables 2 and 3, illustrating that the proposed Eq. (20) provides satisfactory
415 simulations with $R^2 = 0.98$.

416 It is worth noting that as the coarse grain content f_v = 0% was obtained for soils 6-12, the
417 proposed model (Eq. (21)) could not be used to demonstrate the effect of f_v on M_r. It should
418 be mentioned that previous studies were difficult to be used for validating Eq. (21), because
419 Eq. (21) was proposed based on the variations of $M_{r\text{-}sat}$ with f_v for soils 1-5 (Fig. 6), where the
420 fine soil fraction was kept constant at $\rho_{dmax\text{-}f}$ = 1.82 Mg/m^3 (leading to a constant ψ for
421 mixture), whatever the f_v values (as shown in Fig. 2). However, in previous studies, the ρ_d of
422 mixture was generally kept constant. In that case, an increase of f_v led to a decrease of the dry
423 density of fine soil fraction $\rho_{d\text{-}f}$ and thus a decrease of ψ.

424 Table 5. Values of model parameters in the proposed Eq. (20) for soils 1-12

Reference	Soil. No	α_1	β_1	R^2
Wang et al. [3] and Su et al. [7]	1	-1.390	0.967	0.90
	2			0.98
	3			0.96
	4			0.92
	5			0.92
Zaman and Khoury [37]	6	0	2.891	0.95
	7			0.95
	8			0.95
Gupta et al. [9]	9	-2.808	1.046	0.98
Ng et al. [12]	10	-4.126	1.535	0.96
Yang et al. [38]	11	-4.928	0.681	0.98
Yang et al. [13]	12	-3.943	1.606	0.98

425

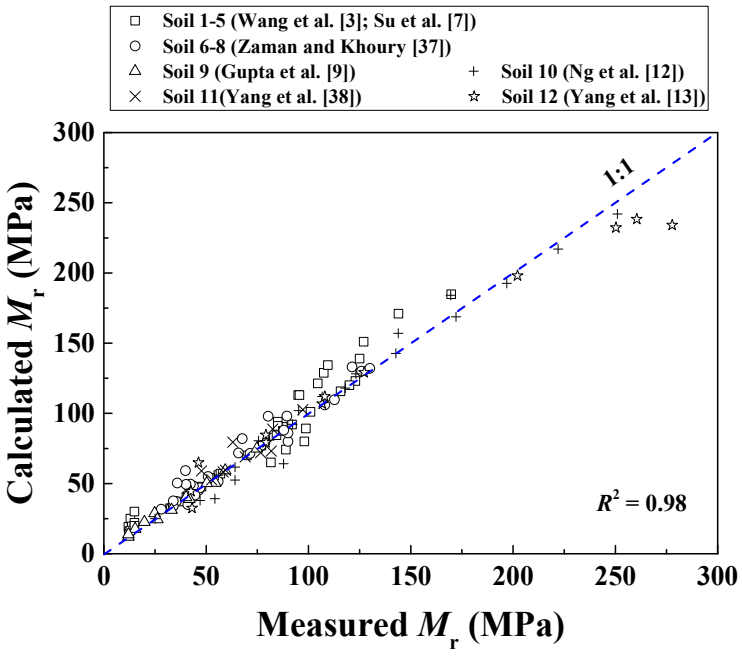

426

427 Fig. 12. Comparison between measured and calculated M_r values for soils 1-12

428

429 COMPARISON BETWEEN THE PROPOSED MODEL AND REPRESENTATIVE
430 EXISTING MODELS

431 To better illustrate the performance of the proposed model, a comparison was made with some
432 representative existing models. According to Han and Vanapalli [17], the constitutive models
433 of M_r could be categorized into three groups: group A - empirical models (e.g. Eqs. (1) - (4)
434 and (9)); group B - models incorporating ψ into deviator or mean stresses (e.g. Eqs. (5) - (6));
435 group C- models considering ψ as an independent term (e.g. Eqs. (7) - (8) and (10)). Three
436 representative models were selected from these three groups: Eq. (9) (ARA, Inc., ERES
437 Consultants Division. [18]), Eq. (5) (Liang et al. [19]) and Eq. (10) (Han and Vanapalli [14])
438 for groups A, B and C, respectively. Note that Eqs. (9) - (10) incorporated SWRC using Eq.
439 (17). Three studies were adopted for the comparison among (Table 6): soil 10 (Ng et al. [12])

of category I ($\psi < \psi_{th}$), soil 12 (Yang et al. [13]) of category II ($\psi > \psi_{th}$ and $\psi_{th} < \psi_{opt}$) and soil 5 (Wang et al. [3]; Su et al. [7]) of category II ($\psi > \psi_{th}$ and $\psi_{th} > \psi_{opt}$).

Table 6. Model parameters for three representative existing models

Equation/Parameter	Category I: $\psi < \psi_{th}$	Category II: $\psi > \psi_{th}$					
	Soil 10	$\psi_{th} < \psi_{opt}$	$\psi_{th} > \psi_{opt}$				
		Soil 12	Soil 1	Soil 2	Soil 3	Soil 4	Soil 5
Eq. (9)							
a	-0.593	-0.593					
b	0.400	0.400					
k_m	6.132	6.132			—		
R^2	0.94	0.72					
Eq. (5)							
k_4	0.453	0.513					
k_5	3.287	1.337					
k_6	-6.887	-1.303			—		
R^2	0.97	0.75					
Eq. (10)							
ξ	1.092	0.983	1.105	0.846	0.714	0.637	0.423
R^2	0.92	0.94	0.88	0.85	0.82	0.68	0.67

Fig. 13(a) shows the M_r measured by Ng et al. [12] and that calculated by Eq. (9) using parameters a = -0.593, b = 0.400 and k_m = 6.132. A reasonably good agreement was obtained between the measurements and the calculations (R^2 = 0.94). The similar phenomenon was observed in Figs. 13(b) - (c): Eqs. (5) and (10) provided satisfactory simulations with parameters presented in Table 6 (R^2 = 0.97 and 0.92, respectively). This indicates that in the case of category I ($\psi < \psi_{th}$), all the three representative existing models as well as the proposed Eq. (20) can be used to describe the M_r variations.

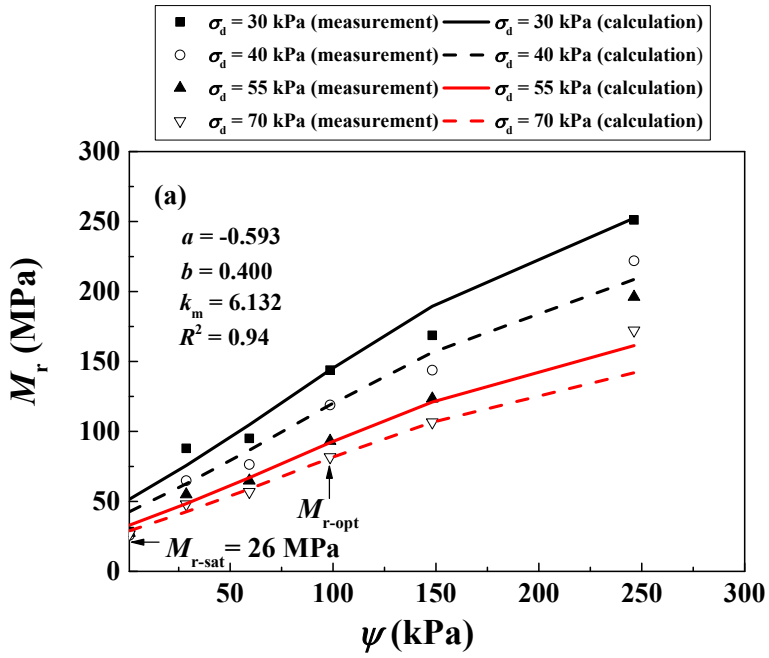
σd = 30 kPa (measurement)
σd = 30 kPa (calculation)
σd = 40 kPa (measurement)
σd = 40 kPa (calculation)
σd = 55 kPa (measurement)
σd = 55 kPa (calculation)
σd = 70 kPa (measurement)
σd = 70 kPa (calculation)
(a)
a = -0.593
b = 0.400
km = 6.132
R2 = 0.94
Mr-opt
Mr-sat = 26 MPa
Mr (MPa)
ψ (kPa)
0
50
100
150
200
250
300

454

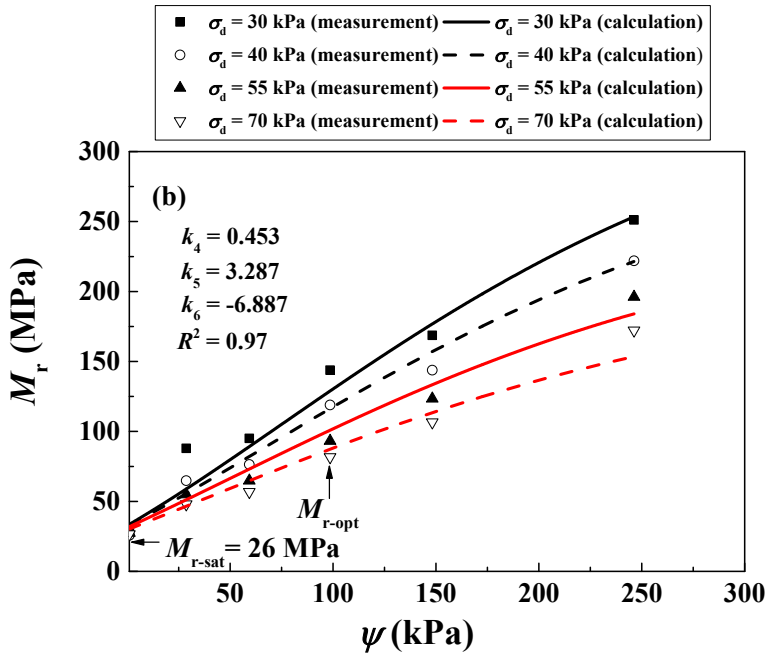

455

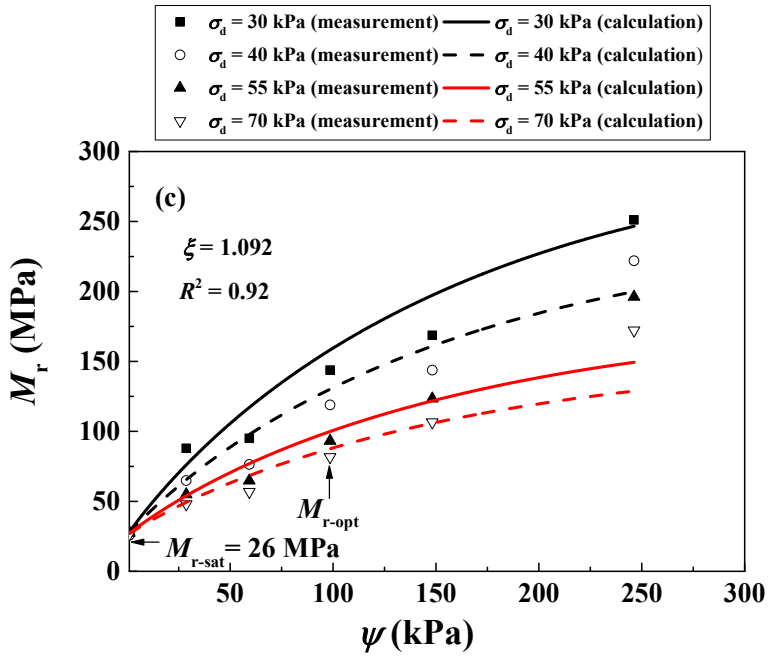

456

457 Fig. 13. Comparisons between the variations of M_r with ψ for soil 10 measured by Ng et al.
458 [12] and those calculated by: (a) Eq. (9) (ARA, Inc., ERES Consultants Division. [20]); (b) Eq.
459 (5) (Liang et al. [21]); (c) Eq. (10) (Han and Vanapalli [14])

460

Fig. 14(a) shows the M_r measured by Yang et al. [13] and that calculated by Eq. (9). Compared with Eq. (20) (the proposed model), Eq. (9) provided less satisfactory simulations: $R^2 = 0.72$ for Eq. (9) against $R^2 = 0.98$ for Eq. (20) (see Fig. 11(b)). More importantly, the ψ_{th} cannot be reproduced by Eq. (9). The similar observations were made from Fig. 14(b) for Eq. (5). On the contrary, Fig. 14(c) shows good simulations by Eq. (10) with $R^2 = 0.94$ using parameter $\xi = 0.983$. Moreover, the ψ_{th} ($< \psi_{opt} = 500$ kPa in Yang et al. [13]) was identified, separating the ψ into two zones with different effects of σ_d. This indicates that in the case of category II ($\psi > \psi_{th}$ and $\psi_{th} < \psi_{opt}$), among the three representative models, only Eq. (10) can be used describe the M_r variations.

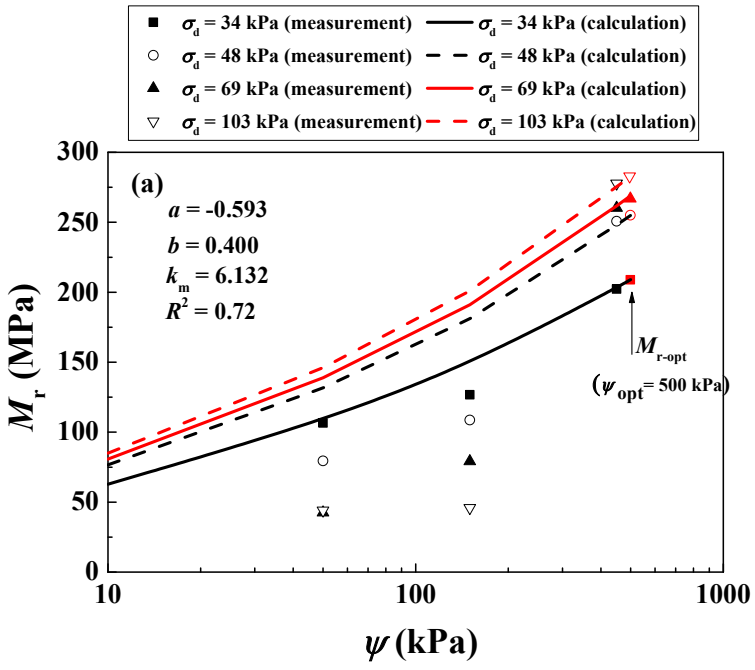

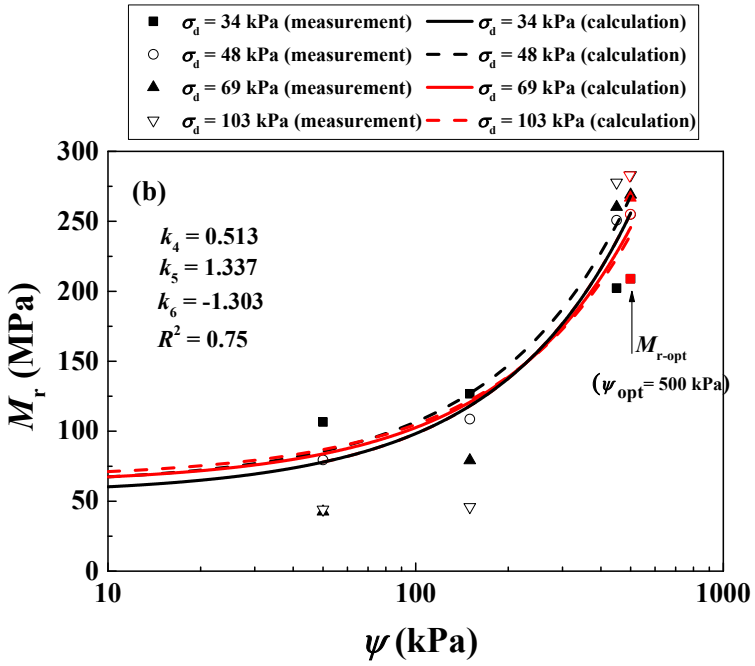

472

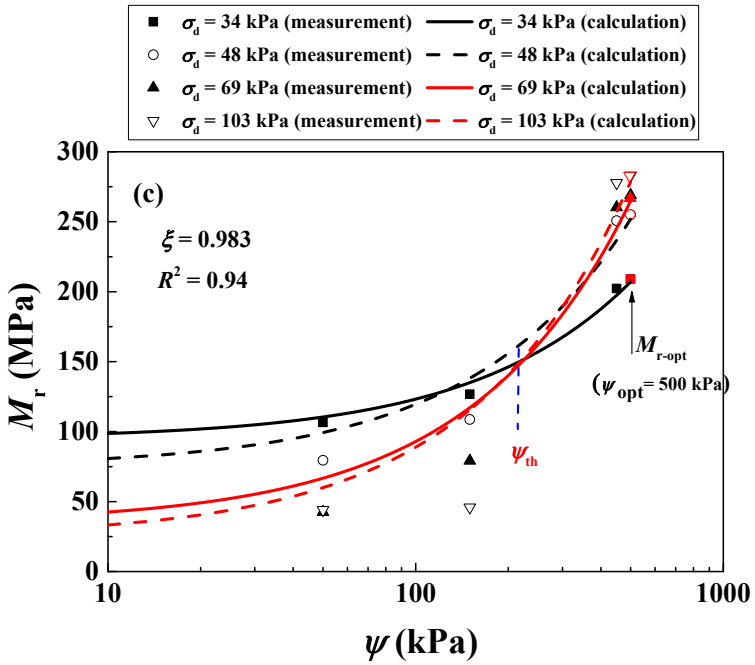

473

474 Fig. 14. Comparisons between the variations of M_r with ψ for soil 12 measured by Yang et al.
475 [13] and those calculated by: (a) Eq. (9) (ARA, Inc., ERES Consultants Division. [20]); (b) Eq.
476 (5) (Liang et al. [21]); (c) Eq. (10) (Han and Vanapalli [14])

477

Fig. 15 shows the comparisons between the M_r measured by Wang et al. [3] and Su et al. [7] and that calculated by Eq. (10) for soils 1-5. Since Eqs. (5) and (9) cannot fit well for soil 12 of category II ($\psi_{th} < \psi_{opt}$, see details in Figs. 14(a) - (b)), they were excluded for soils 1-5 of category II ($\psi_{th} > \psi_{opt}$). Figs. 15(a) - (e) show that Eq. (10) provides simulation results with R^2 = 0.88, 0.85, 0.82, 0.68 and 0.67, smaller than R^2 = 0.90, 0.98, 0.96, 0.92 and 0.92 by the proposed Eq. (20) for soils 1-5 respectively. Moreover, the increase of σ_d led to a decrease of calculated M_r by Eq. (10) in the full ψ range, without identifying ψ_{th}. This indicated that Eq. (10) is not suitable for the case of category II ($\psi_{th} > \psi_{opt}$). This can be explained by the consideration of two reference M_r values- $M_{r\text{-}sat}$ and $M_{r\text{-}opt}$ in Eq. (10). Indeed, through such consideration, the variation of M_r from the saturated condition to the OMC condition (ψ varies from 0 to ψ_{opt}) is expected to be well depicted (see Fig. 14 (c)). However, when $\psi_{th} > \psi_{opt}$, the good description of Eq. (10) is no longer guaranteed (see Fig. 15).

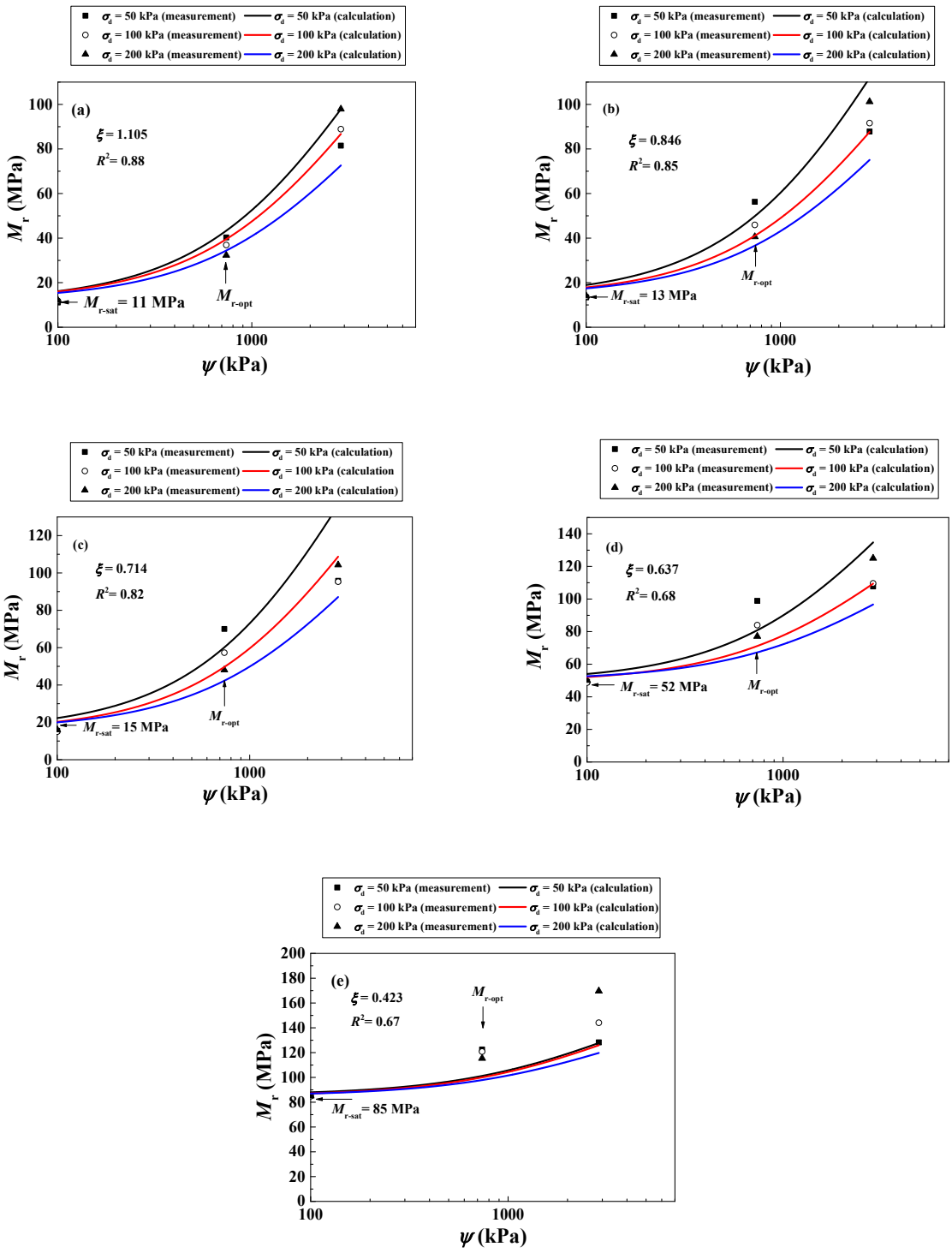

494

495 Fig. 15. Comparisons between the variations of M_r with ψ for soils 1 - 5 measured by Wang et
496 al. [3] and Su et al. [7] and those calculated by Eq. (10) (Han and Vanapalli [14]): (a) soil 1 at
497 f_v = 0%; (b) soil 2 at f_v = 10%; (c) soil 3 at f_v = 20%; (d) soil 4 at f_v = 35%; (e) soil 5 at f_v =
498 45%

499 The comparison of different models indicates that the variation of M_r can be well
500 described by Eqs. (9), (5) and (10) from group A, B and C for category I ($\psi < \psi_{th}$). For
501 category II ($\psi_{th} < \psi_{opt}$), only Eq. (10) among the three representative models can give
502 satisfactory description, while for category II ($\psi_{th} > \psi_{opt}$), even Eq. (10) fails. This leads to
503 the conclusion that only the proposed Eq. (20) which incorporates the combined effects of σ_d
504 and ψ on the M_r in the full range of suction can provide good description for both $\psi_{th} < \psi_{opt}$
505 and $\psi_{th} > \psi_{opt}$.

506 It is worth noting that as the existing models incorporating SWRC, such as Eq. (10) (Han
507 and Vanapalli [14]), the hysteresis effect has not been accounted for. Further studies are
508 needed to extend the proposed model to the hysteresis effect.

509

510 CONCLUSIONS

511 A constitutive model was proposed to describe the variation of resilient modulus M_r with
512 suction ψ and deviator stress σ_d. This model was then extended to the effect of coarse grain
513 content f_v based on the experimental data from Wang et al. [3] and Su et al. [7] to describe the
514 variation of M_r for unsaturated fine/coarse soil mixtures. The model incorporates soil-water
515 retention curve (SWRC). The key parameters are the resilient modulus at saturated sate $M_{r\text{-}sat}$,
516 the resilient modulus at optimum state $M_{r\text{-}opt}$, the suction at optimum state ψ_{opt}, soil parameters
517 α_1 and β_1, as well as the parameters related to SWRC. The proposed model was validated
518 using five different studies. A comparative study was also conducted between the proposed

519 model and three representative existing models from literature. The following conclusions can
520 be drawn:

521 The effect of σ_d on M_r was found to be highly dependent on ψ, with a threshold suction
522 ψ_{th} separating ψ into two zones: with an increasing σ_d, the M_r decreased at $\psi < \psi_{th}$, while
523 increased at $\psi > \psi_{th}$. Using the threshold suction $\psi_{th,}$ previous studies from literature could
524 be divided into two categories: category I ($\psi < \psi_{th}$) and category II ($\psi > \psi_{th}$). For category I
525 ($\psi < \psi_{th}$), the variation of M_r could be satisfactorily described by the three representative
526 models. For category II ($\psi > \psi_{th}$), only Eq. (10) among the three representative models
527 provided satisfactory simulations in the case of $\psi_{th} > \psi_{opt}$. However, in the case of $\psi_{th} < \psi_{opt}$,
528 Eq. (10) failed also. Unlike the three representative models, the proposed model Eq. (20)
529 could gave good results in the full ψ range. In addition, the effect of f_v was well incorporated
530 using Eq. (21). Thus, the proposed model constitutes a helpful tool for describing the variation
531 of resilient modulus of unsaturated fine/coarse soil mixtures under the combined effects of
532 deviator stress and suction.

533

534 ACKNOWLEDGEMENTS

535 This work was supported by China Scholarship Council (CSC) and Ecole des Ponts ParisTech.

536

537 NOTATIONS

f_v	coarse grain content
$f_{v\text{-}cha}$	characteristic coarse grain content

G_s	specific gravity
I_P	plasticity index
M_r	resilient modulus
$M_{r\text{-}sat}$	resilient modulus at saturation condition
$M_{r\text{-}opt}$	resilient modulus at optimum moisture content condition
M_0	$M_{r\text{-}sat}$ at f_v = 0%
M_1	$M_{r\text{-}sat}$ at f_v = 100%
ρ_d	dry density of soil mixture
$\rho_{dmax\text{-}f}$	maximum dry density of fine soil
S_r	degree of saturation
$S_{r\text{-}r}$	residual degree of saturation
$S_{r\text{-}opt}$	degree of saturation at optimum moisture content condition
S_r^e	effective degree of saturation
S_{r-opt}^e	effective degree of saturation at optimum moisture content condition
w	water content of soil mixture
$w_{opt\text{-}f}$	optimum water content of fine soil
w_f	water content of fine soil
w_L	liquid limit
ψ	suction
ψ_{opt}	suction at optimum water content condition
ψ_{th}	threshold suction
θ_b	bulk stress
τ_{oct}	octahedral shear stress
χ	Bishop's effective stress parameter
σ_d	deviator stress

538

539

540

541

542 REFERENCES

543 [1] Trinh, V. N. (2011). Comportement hydromécanique des matériaux constitutifs de
544 plateformes ferroviaires anciennes. PhD Thesis, Ecole Nationale des Ponts et
545 Chaussées, Université Paris-Est.

546 [2] Nie, R., Li, Y., Leng, W., Mei, H., Dong, J., & Chen, X. (2020). Deformation
547 characteristics of fine-grained soil under cyclic loading with intermittence. Acta
548 Geotechnica, 1-14.

549 [3] Wang, H. L., Cui, Y. J., Lamas-Lopez, F., Dupla, J. C., Canou, J., Calon, N., & Chen,
550 R. P. (2017). Effects of inclusion contents on resilient modulus and damping ratio of
551 unsaturated track-bed materials. Canadian Geotechnical Journal, 54(12), 1672-1681.

552 [4] Wang, H.L., Cui, Y.J., Lamas-Lopez, F., Calon, N., Saussine, G., Dupla, J.C., Canou,
553 J., Aimedieu, P. and Chen, R.P., (2018a). Investigation on the mechanical behavior of
554 track-bed materials at various contents of coarse grains. *Construction and Building*
555 *Materials*, *164*, pp.228-237.

556 [5] Wang, H.L., Cui, Y.J., Lamas-Lopez, F., Dupla, J.C., Canou, J., Calon, N., Saussine,
557 G., Aimedieu, P. and Chen, R.P., (2018b). Permanent deformation of track-bed
558 materials at various inclusion contents under large number of loading cycles. *Journal*
559 *of Geotechnical and Geoenvironmental Engineering*, *144*(8), p.04018044.

[6] Qi, S., Cui, Y.J., Chen, R.P., Wang, H.L., Lamas-Lopez, F., Aimedieu, P., Dupla, J.C., Canou, J. and Saussine, G., (2020). Influence of grain size distribution of inclusions on the mechanical behaviours of track-bed materials. Géotechnique, 70(3), pp.238-247.

[7] Su, Y., Cui, Y. J., Dupla, J. C., & Canou, J. (2021a). Effect of water content on resilient modulus and damping ratio of fine/coarse soil mixture with varying coarse grain contents. Transportation Geotechnics, 100452.

[8] Cui, Y. J. (2018). Mechanical behaviour of coarse grains/fines mixture under monotonic and cyclic loadings. Transportation Geotechnics, 17, 91-97.

[9] Gupta, S., Ranaivoson, A., Edil, T., Benson, C., & Sawangsuriya, A. (2007). Pavement design using unsaturated soil technology.

[10] Nowamooz, H., Chazallon, C., Arsenie, M. I., Hornych, P., & Masrouri, F. (2011). Unsaturated resilient behavior of a natural compacted sand. Computers and Geotechnics, 38(4), 491-503.

[11] Gu, C., Zhan, Y., Wang, J., Cai, Y., Cao, Z., & Zhang, Q. (2020). Resilient and permanent deformation of unsaturated unbound granular materials under cyclic loading by the large-scale triaxial tests. Acta Geotechnica, 15(12), 3343-3356.

[12] Ng, C. W. W., Zhou, C., Yuan, Q., & Xu, J. (2013). Resilient modulus of unsaturated subgrade soil: experimental and theoretical investigations. Canadian Geotechnical Journal, 50(2), 223-232.

580 [13] Yang, S. R., Lin, H. D., Kung, J. H., & Huang, W. H. (2008). Suction-controlled
581 laboratory test on resilient modulus of unsaturated compacted subgrade soils. Journal
582 of Geotechnical and Geoenvironmental Engineering, 134(9), 1375-1384.
583 [14] Han, Z., & Vanapalli, S. K. (2015). Model for predicting resilient modulus of
584 unsaturated subgrade soil using soil-water characteristic curve. Canadian Geotechnical
585 Journal, 52(10), 1605-1619.
586 [15] Oh, W. T., Vanapalli, S. K., & Puppala, A. J. (2009). Semi-empirical model for the
587 prediction of modulus of elasticity for unsaturated soils. Canadian Geotechnical
588 Journal, 46(8), 903-914.
589 [16] Han, Z., & Vanapalli, S. K. (2016a). Stiffness and shear strength of unsaturated soils
590 in relation to soil-water characteristic curve. Géotechnique, 66(8), 627-647.
591 [17] Han, Z., & Vanapalli, S. K. (2016b). State-of-the-Art: Prediction of resilient modulus
592 of unsaturated subgrade soils. International Journal of Geomechanics, 16(4), 04015104.
593 [18] Sawangsuriya, A., Edil, T. B., & Benson, C. H. (2009). Effect of suction on resilient
594 modulus of compacted fine-grained subgrade soils. Transportation research record,
595 2101(1), 82-87.
596 [19] Ba, M., Nokkaew, K., Fall, M., & Tinjum, J. M. (2013). Effect of matric suction on
597 resilient modulus of compacted aggregate base courses. Geotechnical and Geological
598 Engineering, 31(5), 1497-1510.
599 [20] ARA, Inc., ERES Consultants Division. (2004). Guide for mechanistic - empirical
600 design of new and rehabilitated pavement structures. Final report, NCHRP Project 1-
601 37A. Transportation Research Board, Washington, D.C.

602 [21] Liang, R. Y., Rabab'ah, S., & Khasawneh, M. (2008). Predicting moisture-dependent
603 resilient modulus of cohesive soils using soil suction concept. Journal of
604 Transportation Engineering, 134(1), 34-40.
605 [22] Heath, A. C., Pestana, J. M., Harvey, J. T., & Bejerano, M. O. (2004). Normalizing
606 behavior of unsaturated granular pavement materials. Journal of Geotechnical and
607 Geoenvironmental Engineering, 130(9), 896-904.
608 [23] Khoury, N., Brooks, R., Boeni, S. Y., & Yada, D. (2013). Variation of resilient
609 modulus, strength, and modulus of elasticity of stabilized soils with postcompaction
610 moisture contents. Journal of Materials in Civil Engineering, 25(2), 160-166.
611 [24] Alonso, E. E., Pereira, J. M., Vaunat, J., & Olivella, S. (2010). A microstructurally
612 based effective stress for unsaturated soils. Géotechnique, 60(12), 913-925.
613 [25] Lu, N., Godt, J. W., & Wu, D. T. (2010). A closed - form equation for effective stress
614 in unsaturated soil. Water Resources Research, 46(5).
615 [26] Moossazadeh, J., & Witczak, M. W. (1981). Prediction of subgrade moduli for soil
616 that exhibits nonlinear behavior. Transportation Research Record, (810).
617 [27] Van Genuchten, M. T. (1980). A closed - form equation for predicting the hydraulic
618 conductivity of unsaturated soils. Soil science society of America journal, 44(5), 892-
619 898.
620 [28] Su, Y., Cui, Y. J., Dupla, J. C., & Canou, J. (2021). Soil-water retention behaviour of
621 fine/coarse soil mixture with varying coarse grain contents and fine soil dry densities.
622 Canadian Geotechnical Journal, (ja).

623 [29] Su, Y., Cui, Y.J., Dupla, J.C., Canou, J., Qi, S., (2021b). Developing a sample
624 preparation approach to study the mechanical behavior of unsaturated fine/coarse soil
625 mixture. Geotechnical Testing Journal. https://doi.org/10.1520/GTJ20190450.
626 [30] Cui, Y. J., & Delage, P. (1996). Yielding and plastic behaviour of an unsaturated
627 compacted silt. Géotechnique, 46(2), 291-311.
628 [31] Ng, C. W. W., Baghbanrezvan, S., Sadeghi, H., Zhou, C., & Jafarzadeh, F. (2017).
629 Effect of specimen preparation techniques on dynamic properties of unsaturated fine-
630 grained soil at high suctions. Canadian Geotechnical Journal, 54(9), 1310-1319.
631 [32] Werkmeister, S., Dawson, A. R., & Wellner, F. (2004). Pavement design model for
632 unbound granular materials. Journal of Transportation Engineering, 130(5), 665-674.
633 [33] Duong, T. V., Cui, Y. J., Tang, A. M., Dupla, J. C., Canou, J., Calon, N., & Robinet, A.
634 (2016). Effects of water and fines contents on the resilient modulus of the interlayer
635 soil of railway substructure. Acta Geotechnica, 11(1), 51-59.
636 [34] Qi, S., Cui, Y. J., Dupla, J. C., Chen, R. P., Wang, H. L., Su, Y., ... & Canou, J. (2020).
637 Investigation of the parallel gradation method based on the response of track-bed
638 materials under cyclic loadings. Transportation Geotechnics, 24, 100360.
639 [35] Vallejo, L. E., & Mawby, R. (2000). Porosity influence on the shear strength of
640 granular material–clay mixtures. Engineering Geology, 58(2), 125-136.
641 [36] Su, Y., Cui, Y. J., Dupla, J. C., & Canou, J. (2020). Investigation of the effect of water
642 content on the mechanical behavior of track-bed materials under various coarse grain
643 contents. Construction and Building Materials, 263, 120206.

644 [37] Zaman, M., & Khoury, N. (2007). Effect of soil suction and moisture on resilient
645 modulus of subgrade soils in Oklahoma (No. ORA 125-6662).
646 [38] Yang, S. R., Huang, W. H., & Tai, Y. T. (2005). Variation of resilient modulus with
647 soil suction for compacted subgrade soils. Transportation Research Record, 1913(1),
648 99-106.
649 [39] Delage, P., Audiguier, M., Cui, Y.J. and Howat, M.D., (1996). Microstructure of a
650 compacted silt. *Canadian Geotechnical Journal*, *33*(1), pp.150-158.
651 [40] Vanapalli, S. K., Fredlund, D. G., & Pufahl, D. E. (1999). The influence of soil
652 structure and stress history on the soil–water characteristics of a compacted till.
653 Geotechnique, 49(2), 143-159.
654 [41] Yang, S. R., Kung, J. H., Huang, W. H., & Lin, H. D. (2006). Resilient modulus of
655 unsaturated cohesive subgrade soils. Yantu Gongcheng Xuebao(Chinese Journal of
656 Geotechnical Engineering), 28(2), 225-229.

657

658 LIST OF TABLES

659

LIST OF FIGURES

660

661